Cumulates and gabbros in southern Albanian ophiolites: their bearing on regional tectonic setting

F. KOLLER[1], V. HOECK[2], T. MEISEL[3], C. IONESCU[4], K. ONUZI[5] & D. GHEGA[5]

[1]*Department of Geological Sciences, University of Vienna, Geozentrum, Althanstr. 14, A-1090 Vienna, Austria*

[2]*Department of Geography, Geology and Mineralogy, University of Salzburg, Hellbrunnerstr. 34, A-5020 Salzburg, Austria (e-mail: volker.hoeck@sbg.ac.at)*

[3]*Institute of General and Analytical Chemistry, University of Leoben, A-8700 Leoben, Austria*

[4]*Department of Geology, Babes-Bolyai University, 1 Kogalniceanu Str., RO-400084 Cluj-Napoca, Romania*

[5]*Institute of Geological Research, Blloku Vasil Shanto, Tirana, Albania*

Abstract: The western belt of the southern Albanian ophiolites consists of six major ophiolite massifs (Voskopoja, Rehove, Morava, Devolli, Vallamara, Shpati) and two smaller ones (Luniku and Stravaj). Each massif has a distinct sequence of mantle tectonites, ultramafic cumulates (plagioclase-bearing peridotites and wehrlites), cumulate gabbros, troctolites and isotropic gabbros. Voskopoja, Rehove and Morava have predominantly lherzolites as mantle tectonites, Shpati lherzolites and harzburgites, and Devolli and Vallamara almost exclusively harzburgites. A volcanic section together with volcanogenic sediments occurs only in the Voskopoja and Rehove massifs as well as in the smaller Luniku and Stravaj massifs. Whole-rock geochemistry and mineral chemistry suggest a mid-ocean ridge setting for the origin of the cumulates and gabbros from the Voskopoja, Rehove and Morava massifs, with only a minor suprasubduction zone (SSZ) influence. The Shpati massif and the small Luniku massif show mid-ocean ridge (MOR) and SSZ signatures in their plutonic sequences. Cumulates and gabbros from Devolli and Vallamara formed in an SSZ setting. The predominance of MOR-generated crustal rocks and the relatively minor occurrence of SSZ-generated plutonic rocks together with the volcanogenic sediments in the Voskopoja and Rehove massifs are indicative of a back-arc basin origin of the western belt ophiolites above a westward-dipping subduction zone.

The Albanian ophiolites are part of a large NNW–SSE-striking ophiolite zone, which comprises the Dinaric ophiolites as well as some Greek ophiolites such as Pindos, Vourinos and Othris. The total length of this ophiolite zone is *c.* 1000 km, from Croatia in the NNW (e.g. Lugovic *et al.* 1991; Pamić *et al.* 2002) to Argolis (Greece) in the SSE (e.g. Robertson & Shallo 2000; Bortolotti *et al.* 2004). Their Jurassic age is constrained by palaeontological evidence from the sediments on top of the ophiolites, by the age of the metamorphic soles and by age determinations on the intrusive plagiogranite (Bortolotti *et al.* 2004; Dilek *et al.* 2005, and references therein).

The overall setting of these ophiolites in the regional geological framework in Albania has been discussed by earlier workers (Shallo *et al.* 1990; Shallo 1992, 1994; Frasheri *et al.* 1996; Meco & Aliaj 2000; Robertson & Shallo 2000; Bortolotti *et al.* 2004) and is shown in Figure 1, which follows the tectonic zones outlined by Meco & Aliaj (2000). The tectonic zones located west and NW of the Albanian (Mirdita) ophiolites comprise a westward-directed stack of thrust sheets related to the Apulian continental platform. The Sazani and the Kruja zones represent the carbonate platform, and the Ionian zone an intra-continental rift area (Robertson & Shallo 2000). The Krasta (Cukali) zone (Pindos zone in Greece) is the deep-water passive margin of the Apulian platform. It is, in turn, overthrust by the Albanian Alps, the Vermoshi and Gashi zones, platform-related units to the east of the Krasta zone (Meco & Aliaj 2000; Robertson & Shallo 2000). The Korabi zone (Pelagonian zone in Greece), east of the ophiolites, represents a continental fragment comprising a pre-Alpine basement and a Triassic–Jurassic sedimentary cover.

The Albanian ophiolites form a link between the Greek and the Dinaric ophiolites. An

From: ROBERTSON, A. H. F. & MOUNTRAKIS, D. (eds) 2006. *Tectonic Development of the Eastern Mediterranean Region*. Geological Society, London, Special Publications, **260**, 267–299.
0305-8719/06/$15.00

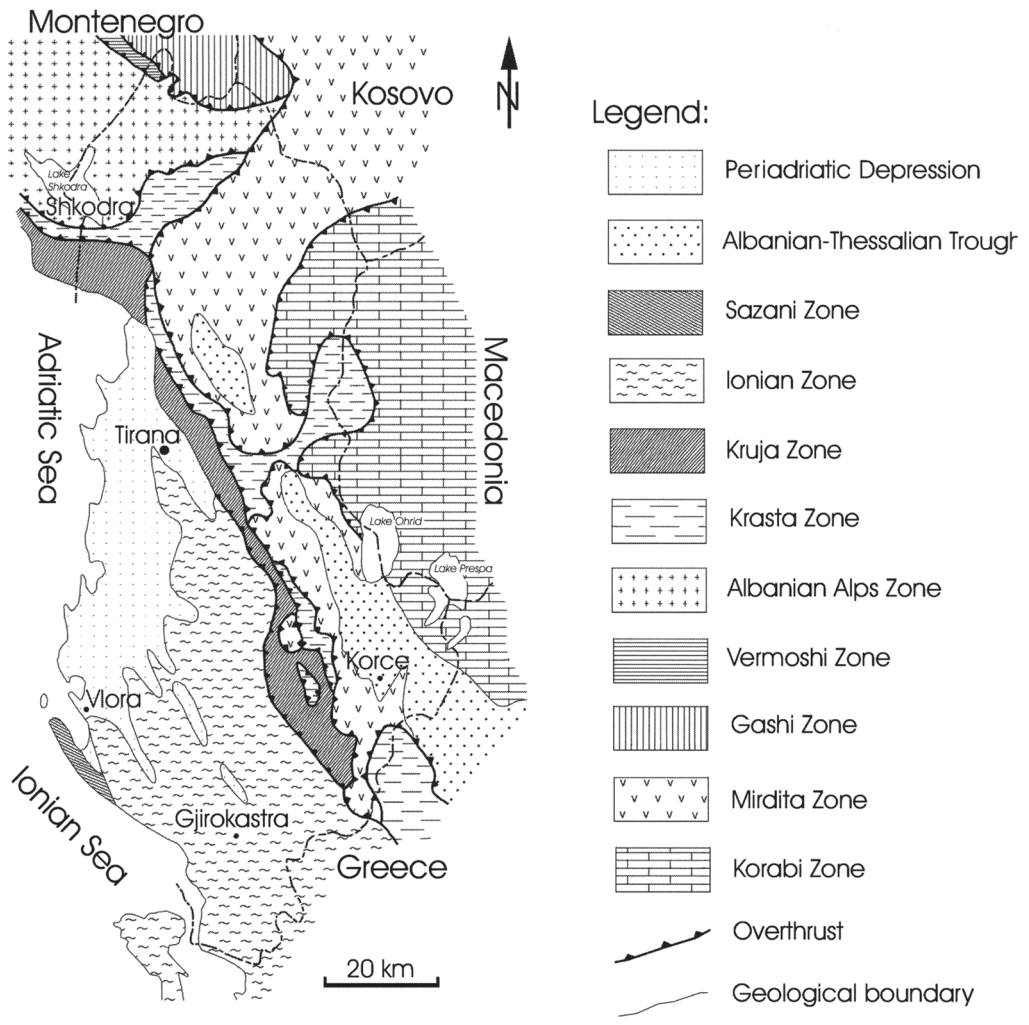

Fig. 1. Overview of the geology of Albania, according to Meco & Aliaj (2000). The various zones are discussed in the text.

understanding of their origin is essential to restore the continent–ocean distribution in the Jurassic in the Eastern Mediterranean realm and the possible sites of subduction zones and related thrusts. As outlined below, the setting of formation of these ophiolites and their mode of emplacement is still controversial.

The Mirdita zone, as delineated in Figure 1, is commonly divided into two ophiolite belts, an eastern one and a western one (e.g. Shallo *et al.* 1990; Shallo 1992, 1994). The western belt is supposed to consist of predominantly mid-ocean ridge (MOR)-type ophiolites with lherzolites, troctolites, gabbros (Cortesogno *et al.* 1998) and MOR-type basalts (MORB). By contrast, the eastern belt is characterized by harzburgites, wehrlites, gabbronorites, clinopyroxene gabbros, plagiogranites and volcanic rocks. These last show a wide range of suprasubduction zone (SSZ) compositions from basalts to andesites, dacites and rhyolites (Shallo 1992, 1994; Beccaluva *et al.* 1994*a*, *b*; Bortolotti *et al.* 1996, 2002, 2004; Robertson & Shallo 2000). Existing models explaining the formation of these contrasting ophiolites infer the presence of intra-oceanic (incipient) subduction zones, involving either east-dipping (Beccaluva *et al.* 1994*b*; Shallo 1994; Bortolotti *et al.* 2002) or west-dipping subduction (Insergueix-Fillippi *et al.* 2000; Robertson & Shallo 2000; Shallo & Dilek 2003; Dilek *et al.* 2005). Based on structural arguments, Nicolas *et al.* (1999) presented a

different concept for the northern Albanian ophiolites, in which both ophiolite belts formed in a slow-spreading MOR setting. The eastern belt would reflect magmatic episodes, whereas, the western belt reflects amagmatic episodes. The mantle tectonites in both belts were originally harzburgites, but in the western belt they were refertilized by basaltic melts to form lherzolites at shallow levels. Recently, Hoeck & Koller (1999), Hoeck *et al.* (2002) and Bortolotti *et al.* (2002) showed that basalts with an SSZ signature also occur in the western belt interlayered with MORB.

In this paper we present evidence that in southern Albania, at least, the SSZ influence known in the western belt is not restricted to the volcanic suite but is also well recorded in the ultramafic tectonites, ultramafic, mafic cumulates, and gabbros. Based on the close spatial and temporal relationship of MOR and SSZ magmas and cumulates, we advocate a back-arc origin for the Albanian ophiolites.

Geological setting

The ophiolites in southern Albania (see ISPGJ–FGJM–IGJN 1983: Geological Map of Albania) are confined to an elongate area ranging from SE of Tirana to the Greek border (Fig. 1). The detailed locations of the ophiolitic massifs are shown in Figure 2. They consist of several units belonging to either the western or the eastern belt. The two belts are separated by the Palaeogene and Neogene molasse sediments of the Neohellenic or Albanian–Thessalian trough (Shallo 1992; Robertson & Shallo 2000; Hoeck *et al.* 2002).

The western belt units (Fig. 2) are, from south to north, the massifs of Voskopoja, Rehove and Morava, below referred to as VRM. The Voskopja and Morava massifs are separated by the north–south-striking Neogene to Quaternary basin of Korce. The Rehove massif is separated from the Morava and Voskopoja massifs by a serpentinite mélange zone, which extends beneath the last two complexes. Towards the north, the Voskopoja massif is followed by the Devolli and Vallamara massifs (referred to as DV below) and furthermore by the Shpati massif with a spur towards the north.

Two additional small massifs, Stravaj, east of Shpati, and, further north, the Luniku massif, crop out as windows beneath the Cenozoic molasse sediments between the two belts (Fig. 2). These are the only massifs containing volcanic rocks apart from Voskopoja and Rehove. A smaller ophiolite body called Erseka, occurring in the south close to the Greek border, is excluded from this study.

The eastern ophiolite belt is represented by the Shebenik massif, which extends from the southern tip of Lake Ohrid towards the north. It is followed further south by the small harzburgitic massifs of Bilisht, south of Lake Prespa (Fig. 2).

Five columnar sections from the western belt including the massifs of Morava, Rehove, Voskopoja, Devolli + Vallamara and Shpati are shown in Figure 3a and b, and characterize the wide lithological variation of these ophiolite bodies. We will discuss first the southern three profiles: Voskopoja, Rehove and Morava (VRM) (Fig. 3a) and subsequently the northern ones: Devolli, Vallamara (DV) and Shpati (Fig. 3b). The total thickness of the ophiolites is indicated in the columnar sections.

Voskopoja, Rehove and Morava sections

Apart from the tectonically underlying mélange, each of these ophiolite sections (Fig. 3a) starts with lherzolites, interlayered with minor harzburgites and rare dunites. Two of the three sections, i.e. Voskopoja and Morava, include a thrust unit within the ultramafic mantle tectonites (the half-arrows in Fig. 3a). A thin layer of amphibolites and metasediments separates a lower thrust unit, consisting only of mantle tectonites, from an upper thrust unit showing a continuous succession with mantle tectonites, cumulates, gabbros and extrusives (only in Voskopoja and Rehove). In Voskopoja, lherzolite of the structurally upper unit contains dykes of completely rodingitized troctolites and rare basalts.

In the Rehove massif, as well in the upper thrust units of the Voskopoja and Morava sections, the ultramafic cumulates commonly include plagioclase wehrlites and minor plagioclase lherzolites followed by cumulate gabbros and troctolites. There are some differences between the three massifs. For example, intrusions of gabbronorites were found only in Morava. In the Rehove section, the ultramafic cumulates are overlain by cumulate gabbros and troctolites. Isotropic gabbros are relatively frequent in Rehove, but rare in Voskopoja and completely missing in Morava. Individual basaltic dykes in the gabbros are widespread in Rehove, rare in Voskopoja and absent in Morava. Sheeted dykes may have been originally present but are not now preserved, except for some remnants occurring together with pillow lavas, only in the Rehove breccias (see below). The ophiolite sequence in Morava ends with the plutonic sequence. Massive basalts are observed

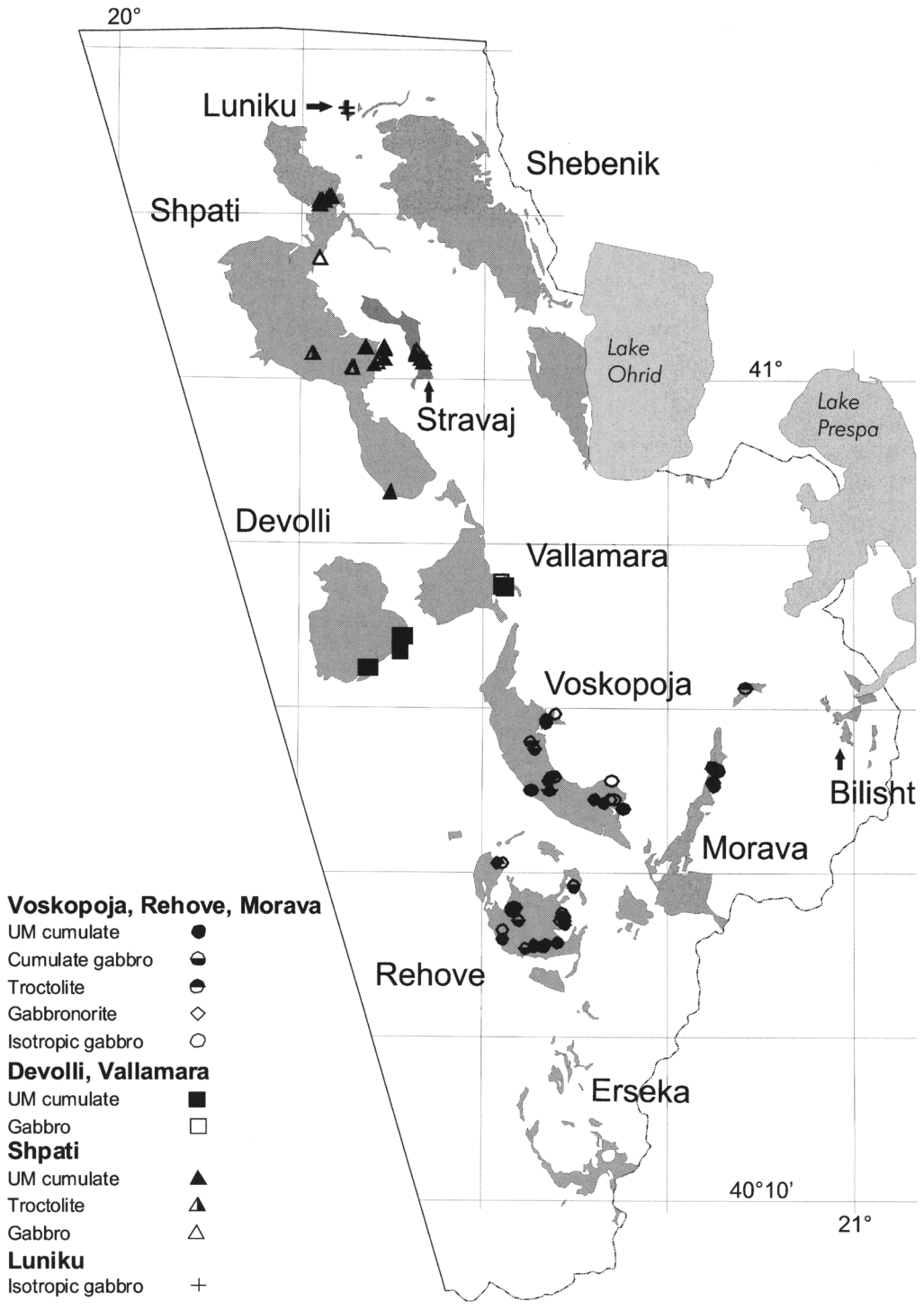

Fig. 2. Sketch map of the south Albanian ophiolite bodies with the sample locations from the individual ophiolite massifs.

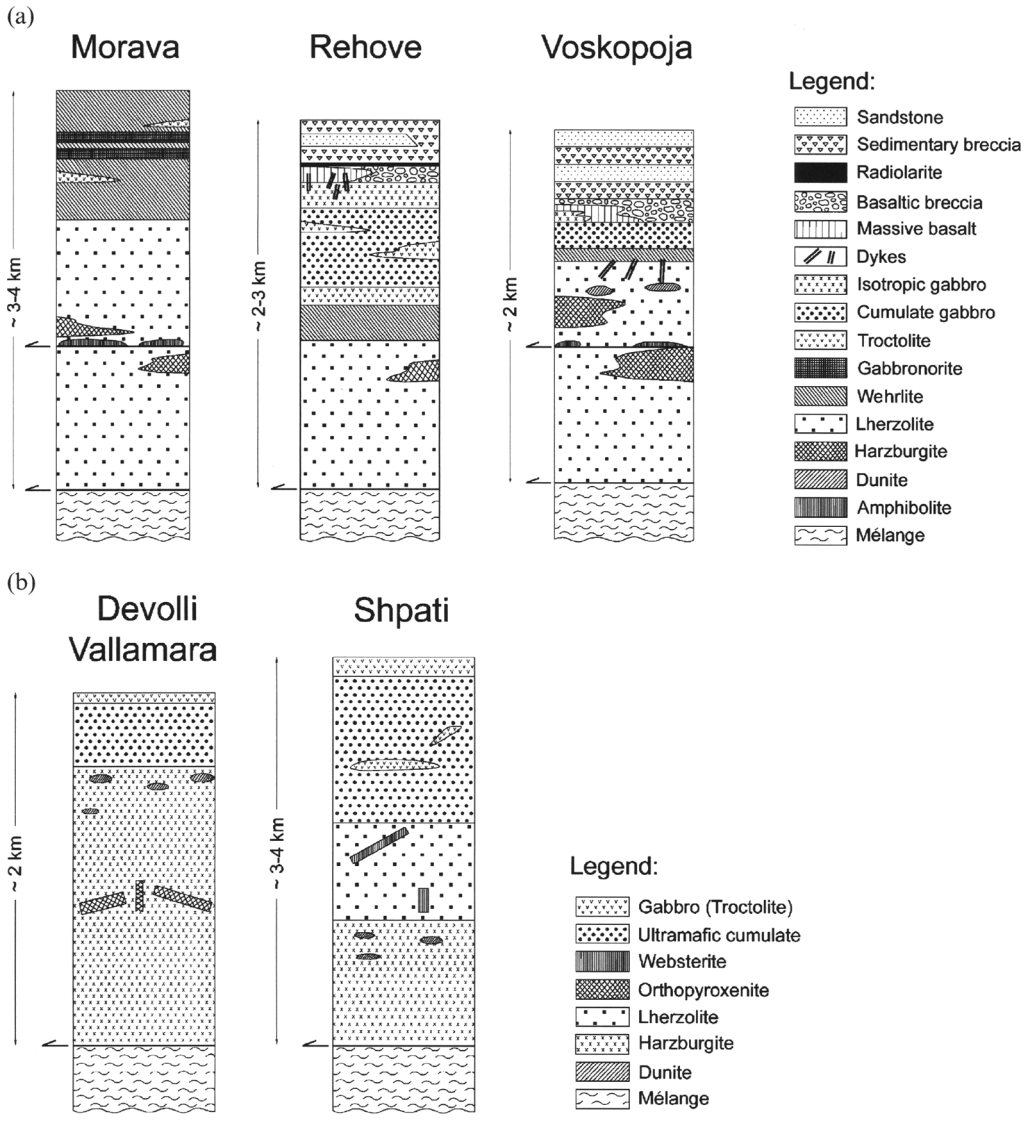

Fig. 3. (**a**) Columnar sections for the Morava, Rehove and Voskopoja massifs based on Hoeck *et al.* (2002). (**b**) Columnar sections for the Devolli + Vallamara and Shpati massifs. The half-arrows indicate thrust planes.

in Rehove as well as in Voskopoja, directly overlying the gabbros, but the most conspicuous and widespread rock types of the extrusive sequence are volcaniclastic sediments. These start with breccias and often finish with volcaniclastic sandstones. (For further details of the extrusive section and the sediments above, see Hoeck *et al.* (2002).)

Devolli, Vallamara and Shpati sections

The Devolli and Vallamara ophioite sections are uniform in their lithology, thus only one columnar section is shown for both (Fig. 3b). In contrast to the western ophiolite bodies they comprise harzburgites but no lherzolites. As in other places, mantle tectonites are underlain tectonically by a mélange containing sediments, serpentinites, minor amphibolites and pillow basalts. Above the tectonic contact follows fresh harzburgite of *c.* 1500–1800 m-thickness, serpentinized only along small fracture zones. Orthopyroxenites, otherwise rare in the western belt, occur frequently as dykes or sills. Dunite lenses are restricted to the upper part of the harzburgites; these are overlain by

plagioclase-bearing peridotites (dunite to lherzolites), representing ultramafic cumulates. In the upper part of the ultramafic cumulates thin gabbro layers (centimetres to decimetres thick) and a few gabbro dykes were observed. A thin cover of gabbros and troctolites, several tens of metres thick, ends the section (Fig. 3b). Extrusive and dyke sections are entirely missing. All of the volcanic rocks mapped in the vicinity of the DV ophiolite body are part of the mélange.

The Shpati massif further north (Fig. 3b) has a section that is intermediate between those of Voskopoja and Rehove on the one hand and Devolli and Vallamara on the other, as it contains a considerable amount of lherzolite. The profile again starts with a mélange with sediments, gabbros and basalts, as well as amphibolites. A metamorphic sole is missing. Tectonically above the mélange are harzburgites with some dunite lenses in the upper part, followed by lherzolites with occasionally websterite dykes and sills. The plagioclase-bearing ultramafic cumulates above the lherzolite contain some layers of troctolites and gabbros in the higher part. Similar to Devolli and Vallamara, the ophiolite section ends with gabbros and rare troctolites. Again, volcanic rocks are missing from the top of the section.

Analytical methods

Geochemical data for the cumulates and gabbros were obtained for 128 samples collected from all of the massifs. These samples comprise a wide variety of lithological types and were taken randomly. After crushing in a metal jaw crusher all samples were ground in an agate mill. Major and trace elements were analysed by X-ray fluorescence (XRF) using a Philips PW 2400 at the Department of Geological Sciences, University of Vienna. For major elements a lithium borate melt pellet and for the trace elements a pressed powder pellet were used. The loss on ignition (LOI) was determined by heating in a furnace at 1000 °C for 3 h. Rare earth elements (REE) and Th, Y, Zr and Nb were analysed by inductively coupled plasma–mass spectrometry (ICP-MS) after microwave assisted (Multiwave Perkin Elmer–Anton Paar) acid digestion with HNO_3–HCl–HF. REE concentrations were determined with external calibration, using a sector field double focusing ICP-MS Element (ThermoFinnigan) system at the Institute of General and Analytical Chemistry, University of Leoben. Some samples were analysed after sodium peroxide sintering with a quadrupole ICP-MS system (at the Institute of General and Analytical Chemistry, University of Leoben) following Meisel *et al.* (2002).

Mineral analyses were carried out on polished thin sections with a JEOL 8600 electron microprobe including a Link control system (at the Department of Geography, Geology and Mineralogy, University of Salzburg). Measurement conditions were 15 kV acceleration voltages and 15 nA beam current. For the quantitative analyses synthetic and natural minerals were used as standards. The correction procedure included the background, dead time and a ZAF calculation built into the Link system.

Petrology of the plutonic section

The main petrographic rock types are ultramafic cumulates that comprise a wide range of compositions including plagioclase dunites, plagioclase peridotites, wehrlites and pyroxenites. They are mostly serpentinized to a variable degree. Where the serpentinization is severe, it is often difficult to differentiate cumulates from the mantle tectonites, refertilized harzburgites or lherzolites. We distinguished the ultramafic cumulates mainly on the basis of visible centimetre- to decimetre-scale layering (Fig. 4) and magmatic textures.

In general, olivine is the first liquidus phase to crystallize; it is often rounded (Fig. 5) and forms small layers in the range of millimetre to centimetre thickness. Very often olivine is partly or completely transformed to serpentine minerals. Cr-spinel forms small, brown, isotropic grains, often showing magmatic resorption. Both olivine and spinel are overgrown by clinopyroxene. When orthopyroxene is present, similar relations are found. Both pyroxenes are concentrated in layers alternating with olivine-rich

Fig. 4. Layering of an ultramafic–mafic cumulate sequence (Morava massif), with layer thickness ranging from 2 and 10 cm.

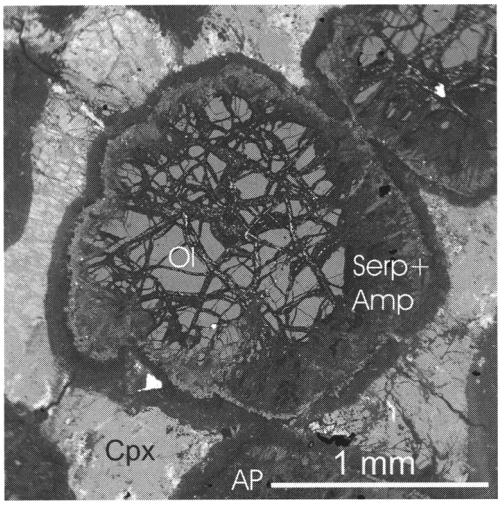

Fig. 5. Back-scattered electron image of a plagioclase-bearing wehrlite from the Rehove massif. Ol, olivine; Cpx, clinopyroxene; Serp + Amp, serpentine and amphibole; AP, altered plagioclase.

layers. Occasionally, clinopyroxene is zoned and shows fine exsolution lamellae of orthopyroxene and, rarely, spinel. Plagioclase is the latest phase to appear, often being associated with a brown amphibole of magmatic(?), origin, with a pargasitic composition. Plagioclase is rarely preserved and was mostly transformed to low-temperature alteration products such as prehnite or hydrogrossular (hibschite to katoite). The dominant sequence of crystallization is olivine + spinel–clinopyroxene/orthopyroxene–plagioclase.

Troctolites and cumulate gabbros differ from the ultramafic cumulates, as plagioclase becomes more dominant and orthopyroxene disappears except for occasional grains. As in the clinopyroxene gabbros, olivine is often rimmed by clinopyroxene, as shown in Figure 6. Olivine and plagioclase constitute troctolites, but with additional clinopyroxene they form cumulate gabbros. Layering is often visible (Fig. 4). There is a transition from ultramafic cumulates to cumulate gabbros and troctolites. As in the ultramafic cumulates, olivine and spinel are often found as inclusions in plagioclase. Inclusions of plagioclase in olivine and clinopyroxene are found as well. Olivine is strongly serpentinized; plagioclase is transformed into low-temperature alteration products, and clinopyroxene is changed to amphiboles. In general, olivine is the first mineral phase to appear, followed by plagioclase and finally clinopyroxene.

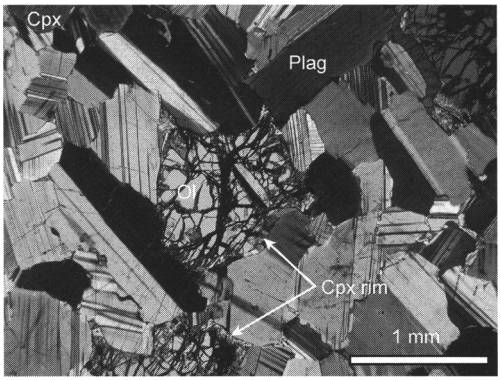

Fig. 6. Thin section of a layered olivine–clinopyroxene gabbro (Voskopoja massif) with olivine (Ol), plagioclase (Plag) and clinopyroxene (Cpx). Olivine is rimmed by clinopyroxene (Cpx rim); crossed Nicols.

The isotropic gabbros and gabbronorites are mostly intrusive and form dykes and stocks in some mafic and ultramafic cumulates, as well as in lherzolites and harzburgites (metres to decametre in size). Particularly in the latter, chloritic intervals may develop at gabbro–ultramafic boundaries. Mineralogically, the isotropic gabbros consist mainly of clinopyroxene and plagioclase, with subordinate olivine. With the exception of gabbronorites in Morava (Fig. 7), orthopyroxene is commonly found, in minor quantities, in the DV and Shpati massifs. The sequence of crystallization is clinopyroxene–orthopyroxene–plagioclase. Most of clinopyroxene is changed to green amphibole with a composition varying from actinolite to magnesiohornblende. Brown magmatic(?) pargasitic amphibole is very rarely present. Plagioclase is also altered; where preserved it is weakly zoned

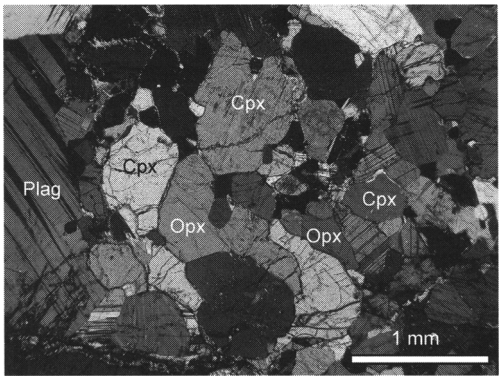

Fig. 7. Thin section of a gabbronorite (Morava massif) with clinopyroxene (Cpx), orthopyroxene (Opx) and plagioclase (Plag); crossed Nicols.

with rims slightly lower in An content than cores. An-poor plagioclase is found only in the vicinity of the secondary amphiboles. Spinels are generally absent; instead, ilmenite and titanomagnetite frequently occur. Isotropic gabbros and gabbronorites reveal the presence of low-temperature alteration products such as albite, prehnite, chlorite and zeolite minerals. Quite commonly, the gabbroic lenses and dykes in the ultramafic rocks and ultramafic cumulates show signs of rodingitization such as increasing Ca content. In these cases, plagioclase is normally replaced by hydrogrossular and prehnite. These oceanic, post-magmatic alteration processes affect mainly the large ion lithophile elements (LILE) and do not influence the high field strength elements (HFSE); this is important for classification.

Mineral chemistry

Olivine (Table 1)

All olivines of the ultramafic and mafic cumulates exhibit a forsterite content of >0.80. In the samples from Voskopoja, Rehove and Morava they show an evolution trend with decreasing X_{Mg} from ultramafic cumulates (0.895–0.881) to cumulate gabbros and troctolites (0.860–0.845). Only one sample of an isotropic gabbro contains olivine with X_{Mg} as low as 0.818 (Fig. 8). MnO increases from 0.1 wt% in the ultramafic cumulates to 0.3 wt% in the gabbros; the NiO content decreases from 0.31 wt% in the ultramafic cumulates to 0.09 wt% in the gabbros. Olivines from the ultramafic cumulates from Devolli and Shpati have higher X_{Mg} values, in the range of 0.900–0.897. Gabbros from Shpati, with X_{Mg} of 0.892, show higher values than the troctolites of the same unit (X_{Mg} 0.875).

Orthopyroxene (Table 2)

This is represented mostly by enstatite. The X_{Mg} varies from 0.845 in an orthopyroxene from a gabbro from Devolli to 0.907 in an ultramafic cumulate also from Devolli and in a cumulate gabbro from Vallamara. The Al_2O_3 content is more variable, ranging from 0.5 to 2.2 wt% in a gabbro from Morava. CaO ranges from 0.6 to 1.4 wt%. A gabbro from Shpati contains pigeonite with X_{Mg} <0.80, CaO from 2.1 to 3.4 wt% and an Al_2O_3 content of 0.4 wt%, significantly lower compared with enstatite.

Clinopyroxene (Table 3)

This is the most widespread mineral in all of the cumulates and gabbros, except where it is completely altered to amphibole (actinolite to magnesiohornblende). As for orthopyroxene, the X_{Mg} is usually very high, with little variation (0.86–0.93). Lower values are found only in the pigeonite-bearing gabbros and in an orthopyroxene-free cumulate gabbro from Rehove (0.765–0.824). All clinopyroxenes from the ultramafic cumulates classify as diopsides, whereas those from the cumulate and isotropic gabbros are diopsides or augites. They differ from clinopyroxene from the ultramafic cumulates by the enrichment in ferrosilite component and a slight depletion in the wollastonite end-member. There is also a significant change in the composition of clinopyroxene in the isotropic gabbros for minor elements such as Al_2O_3, TiO_2, Na_2O and Cr. A covariation of Na and Ti with X_{Mg} is displayed in Figures 9 and 10. Differences can be observed (1) between the ultramafic cumulates and the mafic rocks from the same massif and (2) between the cumulates and gabbros from different massifs.

Several trends can be recognized in the covariation of Ti, Na and Cr (not shown) with X_{Mg} in clinopyroxene. Ti and Na are negatively correlated and Cr is positively correlated with X_{Mg}. At a given concentration of these elements, the X_{Mg} of clinopyroxene from the ultramafic cumulates is normally higher than for the cumulate and isotropic gabbros. The high values of X_{Mg} in each group of clinopyroxene reflect the X_{Mg} of the whole rock.

The ultramafic rocks of DV, Shpati and VRM define a steep trend with high variation of Na and Ti, but little decrease in X_{Mg}. The strong enrichment trend of Ti and, in particular, Na in the ultramafic cumulates from all units is illustrated by a series of samples without a large systematic variation within these samples. No dependence between Na and Ti content in the whole rock and the content of these elements in the clinopyroxene is discernible. By contrast, the cumulate and isotropic gabbro trends mostly show a larger covariation of X_{Mg} with Ti and Na. Most of the samples form small patches with little internal variation of Ti, Na and X_{Mg}. Only two samples, one gabbro from Shpati and one gabbro from Luniku, exhibit perceptible trends with decreasing X_{Mg} and increasing Ti and Na from the cores to the rims. Another gabbro (as well as troctolites from Shpati) shows trends of high Na and X_{Mg} clinopyroxenes, comparable with the ultramafic rocks.

Spinel (Table 4)

Cr-spinel is mostly restricted to the ultramafic cumulates, troctolites and a very few cumulate

Table 1. *Representative olivine analyses from the ultramafic cumulates (UM Cum) and all gabbroic rocks of the southern Albanian ophiolites*

Sample:	99A020	99A98	96A09	99A88	98A01	99A71	03A343	99A121B	03A362	03A353b	02A319	02A280a	02A285A
Massif:	Voskopoja				Rehove		Morava		Devolli	Vallamara	Shpati		
Rock:	UM Cum	UM Cum	Gabbro	Gabbro	Plag-Wehrlite	Troctolite	Plag-Dunite	Troctolite	UM Cum	UM Cum	Plag-Dunite	Gabbro	Troctolite
SiO_2	40.63	40.82	39.23	39.66	40.61	39.87	40.66	39.73	40.74	41.22	41.70	41.42	40.22
TiO_2	0.00	0.01	0.00	0.06	0.03	0.03	0.00	0.00	0.00	0.00	0.01	0.00	0.00
Al_2O_3	0.00	0.01	0.01	0.02	0.01	0.00	0.01	0.00	0.02	0.00	0.01	0.01	0.01
Cr_2O_3	0.02	0.00	0.00	0.01	0.03	0.00	0.01	0.02	0.01	0.02	0.03	0.02	0.00
FeO	11.18	10.71	13.71	17.36	11.23	14.06	10.09	14.74	10.02	9.94	10.33	10.84	11.89
MnO	0.18	0.15	0.20	0.29	0.18	0.27	0.14	0.24	0.12	0.13	0.17	0.12	0.19
NiO	0.30	0.09	0.36	0.06	0.32	0.27	0.39	0.21	0.42	0.41	0.28	0.36	0.30
MgO	47.56	48.60	45.28	43.71	47.82	45.57	48.72	45.20	48.55	49.32	49.04	48.30	47.01
CaO	0.06	0.02	0.00	0.10	0.06	0.08	0.04	0.02	0.01	0.00	0.04	0.01	0.02
Total	99.93	100.41	98.80	101.27	100.28	100.15	100.06	100.15	99.90	101.04	101.60	101.07	99.64
Si	1.003	1.000	0.994	0.994	1.000	0.997	0.998	0.996	1.001	1.001	1.007	1.008	1.000
Al	0.000	0.000	0.000	0.001	0.000	0.000	0.000	0.000	0.001	0.000	0.000	0.000	0.000
Ti	0.000	0.000	0.000	0.001	0.001	0.000	0.000	0.000	0.000	0.000	0.000	0.000	0.000
Cr	0.000	0.000	0.000	0.000	0.001	0.000	0.000	0.000	0.000	0.000	0.001	0.000	0.000
Fe	0.231	0.220	0.290	0.364	0.231	0.294	0.207	0.309	0.206	0.202	0.209	0.221	0.247
Mn	0.004	0.003	0.004	0.006	0.004	0.006	0.003	0.005	0.003	0.003	0.003	0.002	0.004
Ni	0.006	0.002	0.007	0.001	0.006	0.005	0.008	0.004	0.008	0.008	0.006	0.007	0.006
Mg	1.751	1.775	1.710	1.634	1.755	1.698	1.783	1.689	1.779	1.785	1.766	1.753	1.742
Ca	0.002	0.000	0.000	0.003	0.001	0.002	0.001	0.001	0.000	0.000	0.001	0.000	0.001
X_{Mg}	0.884	0.890	0.855	0.818	0.884	0.852	0.896	0.845	0.896	0.898	0.894	0.888	0.876

Formula calculation based on four oxygen atoms.

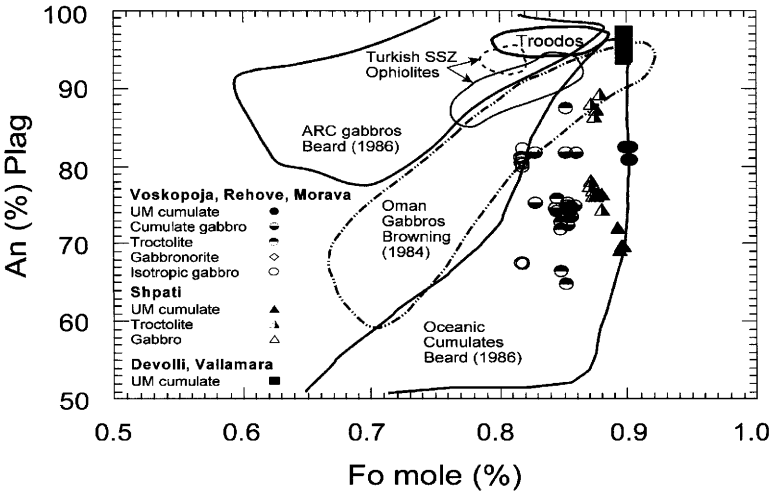

Fig. 8. Fo v. An relations in olivine and plagioclase, respectively. The arc gabbros and oceanic cumulates fields are after Beard (1986); the Turkish SSZ ophiolites field is after Parlak *et al.* (1996, 2000, 2002), and the Troodos ophiolite field is after Hébert & Laurent (1990).

gabbros. Only one isotropic gabbro from Shpati contains Cr-spinel. Spinels from wehrlites in Rehove (Fig. 11) are distinguished by their high Cr-number (0.55–0.62), low Mg-number (0.3–0.5) and high TiO_2 contents (>0.8 wt%). The inset in Figure 11 shows the TiO_2–Al_2O_3 relations (Kamenetsky *et al.* 2001), in which this group overlaps with ocean island basalts. All other spinels show a Cr-number of 0.32–0.55 and an Mg-number between 0.50 and 0.63. In the TiO_2–Al_2O_3 diagram they plot in the MOR field. In particular, Cr-spinels from the Devolli ultramafic cumulates show the highest Mg-number (*c.* 0.63), and the lowest Cr-number (0.32) and TiO_2 contents (<0.2 wt%). Many spinels from the DV and Shpati ultramafic cumulates and a few from VRM show similar Cr-number, Mg-number and TiO_2 contents to the spinels from the mantle harzburgites and lherzolites (Fig. 11). Spinels from the mantle tectonites form a linear array with negatively correlated Cr-number and Mg-number. Harzburgites from Devolli, together with some from VRM, show the highest Cr-number; lower Cr-numbers are shown by the mantle tectonites from VRM and Shpati.

Plagioclase (Table 5)

The An content in the preserved plagioclases ranges from An_{50} in an isotropic gabbro from Shpati to over An_{97} in an ultramafic cumulate from Devolli (Figs 8 and 12). In some samples the variability is much smaller. One sample from the ultramafic cumulates in Morava shows An from 81 to 82, without any significant zoning. Plagioclase with the highest An content of 97 in the core also shows only minor zoning, with a value of 94 at the rim. Plagioclases from the cumulate gabbros, troctolites and isotropic gabbros are commonly zoned, with An-rich cores and An-poor rims. In a cumulate gabbro from Rehove, a plagioclase ranges from An_{77} in the core to An_{58} at the rim. The lowest An content comes from a gabbro at Shpati, with An_{55} in the core and $An_{50.5}$ at the rim. The overall variability is shown in Figure 12. The variation along the An axis in each group illustrates the magmatic zoning between core (high An) and rim (low An).

Geochemistry

Ultramafic cumulates

Analyses of the ultramafic cumulates (plagioclase-bearing dunites, lherzolites and wehrlites) are listed in Table 6. They have a variable composition, which mainly reflects the amount of olivine and plagioclase present. Orthopyroxene and clinopyroxene play a relatively minor role in the geochemical variability (Figs 13a, b and 14a, b). Spinels with a wide range of Cr-number and Mg-number are common accessory phases.

The variability of MgO, Al_2O_3 and CaO is displayed in Figures 13a, b and 14a, b. The Al_2O_3 content is generally <4 wt%; only in Rehove

Table 2. *Representative orthopyroxene analyses from the ultramafic cumulates (UM Cum) and all gabbroic rocks of the southern Albanian ophiolites*

Sample:	99A98	96A09	03A343	99A120	03A362	03A350	03A353b	03A354	02A280a	02A281	02A285A	02A329
Massif:	Voskopoja		Morava		Devolli		Vallamara		Shpati			Luniku
Rock:	UM Cum	Gabbro	Plag-Dunite	UM Cum	UM Cum	Gabbro	UM Cum	Gabbro	Gabbro	Gabbro	Troctolite	Gabbro
SiO_2	56.41	55.93	56.44	56.15	56.13	56.39	56.20	56.59	57.93	52.33	56.74	55.67
TiO_2	0.25	0.15	0.32	0.24	0.10	0.08	0.11	0.09	0.08	0.30	0.06	0.20
Al_2O_3	1.69	1.49	1.62	1.96	2.08	2.23	2.03	2.12	0.98	0.46	1.21	1.25
Cr_2O_3	0.49		0.31	0.31	0.45	0.18	0.48	0.51	0.09	0.00	0.07	0.15
FeO	7.05	8.98	6.87	6.44	6.75	10.57	7.37	6.58	7.02	21.72	8.08	11.80
MnO	0.14	0.23	0.13	0.16	0.16	0.23	0.13	0.15	0.19	0.58	0.22	0.21
NiO	0.04		0.06	0.06	0.08	0.11	0.02	0.06	0.03	0.01	0.05	0.05
MgO	33.45	32.40	33.93	33.89	33.63	30.39	33.00	33.55	33.94	20.28	33.14	28.60
CaO	0.90	0.51	0.53	0.60	0.52	0.78	0.66	0.63	0.32	3.38	0.51	2.27
Na_2O	0.02	0.00	0.01	0.03	0.00	0.00	0.00	0.00	0.01	0.07	0.00	0.05
K_2O	0.00	0.00	0.01	0.00	0.01	0.01	0.00	0.01	0.00	0.00	0.00	0.00
Total	100.44	99.69	100.24	99.83	99.90	100.97	100.00	100.29	100.61	99.14	100.08	100.23
Si	1.949	1.959	1.950	1.945	1.945	1.963	1.950	1.951	1.988	1.981	1.971	1.974
$Al^{[4]}$	0.051	0.041	0.050	0.055	0.055	0.037	0.050	0.049	0.012	0.019	0.029	0.026
$Al^{[6]}$	0.018	0.021	0.016	0.025	0.030	0.055	0.033	0.037	0.028	0.001	0.021	0.026
Ti	0.007	0.004	0.008	0.006	0.003	0.002	0.003	0.002	0.002	0.009	0.002	0.005
Cr	0.013		0.009	0.008	0.012	0.005	0.013	0.014	0.003	0.000	0.002	0.004
Fe	0.204	0.263	0.199	0.186	0.196	0.308	0.214	0.190	0.201	0.687	0.235	0.350
Mn	0.004	0.007	0.004	0.005	0.005	0.007	0.004	0.004	0.006	0.019	0.006	0.006
Ni	0.001		0.002	0.002	0.002	0.003	0.001	0.002	0.001	0.000	0.001	0.002
Mg	1.723	1.692	1.748	1.750	1.737	1.578	1.707	1.724	1.736	1.144	1.716	1.512
Ca	0.033	0.019	0.020	0.022	0.019	0.029	0.025	0.023	0.012	0.137	0.019	0.086
Na	0.001	0.000	0.001	0.002	0.000	0.000	0.000	0.000	0.001	0.005	0.000	0.003
K	0.000	0.000	0.000	0.000	0.000	0.000	0.000	0.000	0.000	0.000	0.000	0.000
Total	4.004	4.006	4.005	4.006	4.004	3.986	3.999	3.997	3.989	4.003	4.002	3.994
X_{Mg}	0.894	0.865	0.898	0.904	0.899	0.837	0.889	0.901	0.896	0.625	0.880	0.812

Formula calculation based on six oxygen atoms.

Table 3. *Representative clinopyroxene analyses from the ultramafic cumulates (UM Cum) and all gabbroic rocks of the southern Albanian ophiolites*

Sample:	99A020	99A88	98A01	98A05	99A054	00A150	99A028	99A120	99A121B	03A362	03A350	03A354	02A319	02A323	02A285A	02A329
Massif:	Voskopoja		Rehove					Morava		Devolli		Vallamara	Shpati			Luniku
Rock:	UM Cum	Gabbro	Plag-Wehrlite	Plag-Wehrlite	Plag-Wehrlite	Gabbro	Gabbro	UM Cum	Troctolite	UM Cum	Gabbro	Gabbro	Plag-Dunite	Plag-Dunite	Troctolite	Gabbro
SiO_2	52.35	52.55	50.80	51.78	52.40	53.25	52.54	52.44	51.91	52.54	54.35	53.65	53.34	53.00	53.95	53.57
TiO_2	0.35	0.54	1.77	0.92	0.83	0.38	0.52	0.56	0.48	0.23	0.11	0.17	0.79	0.32	0.29	0.27
Al_2O_3	3.52	2.86	3.22	2.90	2.77	2.23	2.95	2.96	3.18	2.79	2.54	2.02	2.79	2.56	2.12	2.24
Cr_2O_3	1.13	0.77	1.24	1.22	1.17	0.41	0.85	0.87	0.72	1.29	0.36	0.52	0.66	0.77	0.36	0.50
FeO	2.28	5.18	4.06	4.06	2.99	5.33	4.84	2.71	4.02	2.24	3.99	2.46	2.85	2.57	2.90	6.75
MnO	0.07	0.12	0.10	0.11	0.08	0.16	0.08	0.06	0.13	0.06	0.10	0.08	0.07	0.07	0.10	0.20
NiO	0.00	0.00	0.04	0.00	0.01	0.04	0.04	0.04	0.03	0.06	0.07	0.03	0.06	0.01	0.02	0.03
MgO	15.78	17.31	17.00	16.75	17.15	18.27	16.88	16.72	16.61	16.63	16.45	17.18	16.41	17.63	17.18	17.22
CaO	23.95	20.82	20.47	21.37	21.22	20.54	20.03	22.84	21.61	23.51	22.51	23.30	22.53	22.74	22.69	19.47
Na_2O	0.42	0.33	0.59	0.52	0.46	0.28	0.32	0.43	0.50	0.26	0.32	0.17	0.49	0.38	0.42	0.30
K_2O	0.00	0.01	0.01	0.00	0.01	0.00	0.00	0.00	0.00	0.01	0.00	0.00	0.01	0.01	0.00	0.00
Total	99.85	100.49	99.29	99.64	99.08	100.88	99.06	99.62	99.18	99.62	100.82	99.57	99.99	100.06	100.04	100.55
Si	1.911	1.914	1.873	1.901	1.921	1.929	1.932	1.917	1.912	1.921	1.962	1.955	1.938	1.926	1.957	1.951
$Al^{[4]}$	0.089	0.086	0.127	0.099	0.079	0.071	0.068	0.083	0.088	0.079	0.038	0.045	0.062	0.074	0.043	0.049
$Al^{[6]}$	0.063	0.037	0.012	0.027	0.041	0.024	0.060	0.044	0.050	0.041	0.070	0.042	0.057	0.035	0.048	0.047
Ti	0.010	0.015	0.049	0.025	0.023	0.010	0.014	0.016	0.013	0.006	0.003	0.005	0.022	0.009	0.008	0.007
Cr	0.033	0.022	0.036	0.035	0.034	0.012	0.025	0.025	0.021	0.037	0.010	0.015	0.019	0.022	0.010	0.014
Fe	0.070	0.158	0.125	0.125	0.092	0.161	0.149	0.083	0.124	0.069	0.121	0.075	0.087	0.078	0.088	0.206
Mn	0.002	0.004	0.003	0.004	0.003	0.005	0.003	0.002	0.004	0.002	0.003	0.003	0.002	0.002	0.003	0.006
Ni	0.000	0.000	0.001	0.000	0.000	0.001	0.001	0.001	0.001	0.002	0.002	0.001	0.002	0.000	0.001	0.001
Mg	0.859	0.940	0.934	0.917	0.937	0.986	0.925	0.911	0.912	0.907	0.885	0.933	0.889	0.955	0.929	0.935
Ca	0.937	0.812	0.808	0.841	0.833	0.797	0.789	0.894	0.853	0.921	0.871	0.910	0.877	0.885	0.882	0.760
Na	0.030	0.024	0.042	0.037	0.033	0.020	0.023	0.031	0.035	0.018	0.022	0.012	0.035	0.027	0.030	0.021
K	0.000	0.000	0.000	0.000	0.000	0.000	0.000	0.000	0.000	0.000	0.000	0.000	0.001	0.000	0.000	0.000
Total	4.002	4.011	4.012	4.011	3.996	4.017	3.989	4.007	4.013	4.003	3.987	3.995	3.989	4.014	3.999	3.997
X_{Mg}	0.925	0.856	0.882	0.880	0.911	0.859	0.862	0.917	0.881	0.930	0.880	0.926	0.911	0.924	0.913	0.820

Formula calculation based on six oxygen atoms.

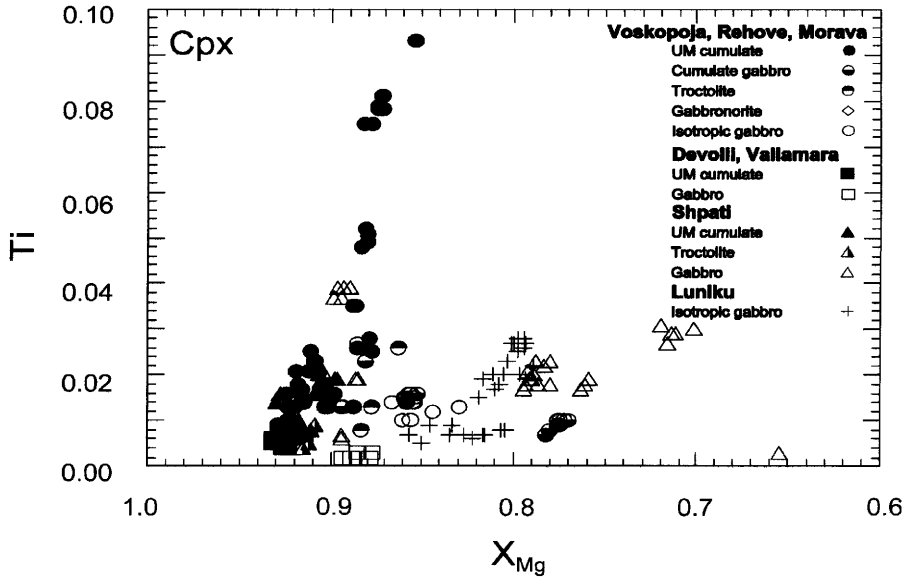

Fig. 9. X_{Mg} v. Ti relations for clinopyroxene from the south Albanian ophiolites.

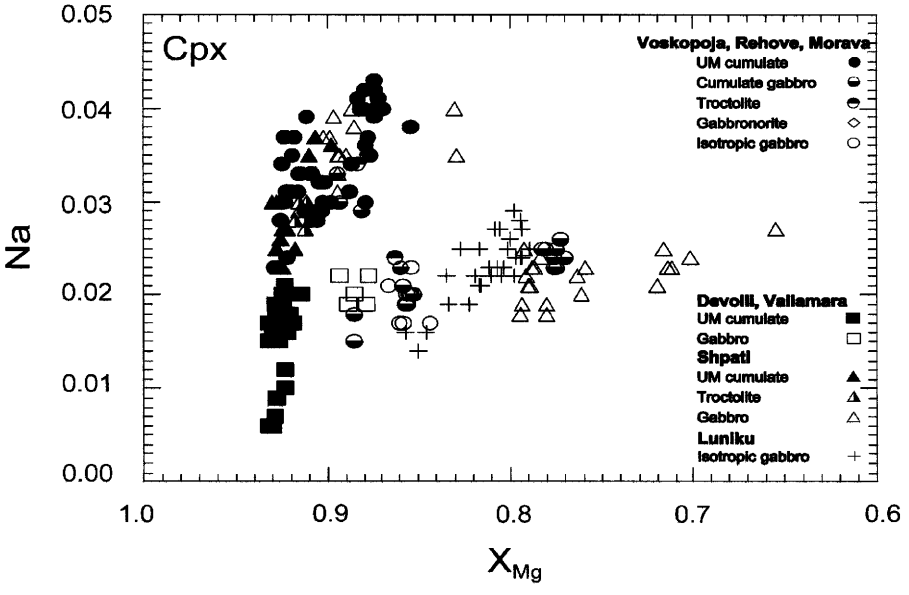

Fig. 10. X_{Mg} v. Na relations for clinopyroxene from the south Albanian ophiolites.

does it exceed 10 wt%. At low Al_2O_3 concentrations, the TiO_2 content is positively correlated with Al_2O_3 in the range between 0.02 and 0.15 wt%. No correlation is observable at higher Al_2O_3 contents, where TiO_2 ranges up to 0.4 wt%. The X_{Mg} expressed as $MgO/(MgO + FeO_{tot})$ is high, at 0.86–0.92 (Fig. 15).

The composition of the ultramafic cumulates with low Al_2O_3 overlaps considerably with that of harzburgites and lherzolites in terms of both major elements and trace elements, such as Cr, Ni or Co. There seems to be only a slight difference in incompatible trace elements (e.g. Y or Zr), in that at least one of these (mostly both) is higher

Table 4. *Representative spinel analyses from the ultramafic cumulates (UM Cum) and all gabbroic rocks of the southern Albanian ophiolites*

Sample:	99A020	99A98	98A01	99A054	99A71	99A120	03A362	03A353b	03A354
Massif:	Voskopoja		Rehove			Morava	Devolli	Vallamara	
Rock:	UM Cum	UM Cum	Plag-Wehrlite	Plag-Wehrlite	Troctolite	UM Cum	UM Cum	UM Cum	Gabbro
TiO_2	0.20	0.96	1.40	1.40	1.38	0.43	0.07	0.16	0.14
Al_2O_3	31.71	19.99	18.45	19.31	18.31	31.17	37.87	31.46	29.67
Cr_2O_3	33.07	41.89	38.92	41.60	39.52	33.54	28.01	34.84	35.02
FeO	21.25	26.98	31.90	26.04	29.59	21.96	17.82	19.83	20.18
MnO	0.27	0.28	0.29	0.29	0.20	0.18	0.17	0.23	0.18
NiO	0.12	0.01	0.18	0.16	0.21	0.11	0.22	0.12	0.12
MgO	12.25	9.46	7.82	10.52	10.16	11.75	14.60	12.54	12.90
Total	98.87	99.57	98.96	99.33	99.36	99.13	98.75	99.18	98.22
Al	1.121	0.749	0.707	0.722	0.688	1.105	1.290	1.109	1.058
Ti	0.005	0.023	0.034	0.034	0.033	0.010	0.001	0.004	0.003
Cr	0.784	1.054	1.000	1.044	0.996	0.798	0.640	0.824	0.838
Fe^{3+}	0.091	0.174	0.259	0.201	0.283	0.087	0.069	0.064	0.101
Fe^{2+}	0.442	0.544	0.608	0.491	0.506	0.466	0.362	0.432	0.410
Mn	0.007	0.008	0.008	0.008	0.005	0.004	0.004	0.006	0.005
Ni	0.003	0.000	0.005	0.004	0.005	0.003	0.005	0.003	0.003
Mg	0.548	0.448	0.379	0.498	0.483	0.527	0.629	0.559	0.582
X_{Mg}	0.553	0.452	0.384	0.504	0.488	0.531	0.635	0.564	0.587
Cr-no.	0.412	0.584	0.586	0.591	0.592	0.419	0.332	0.426	0.442

Formula calculation based on four oxygen atoms. Fe^{3+} calculation based on charge balance within the formula.

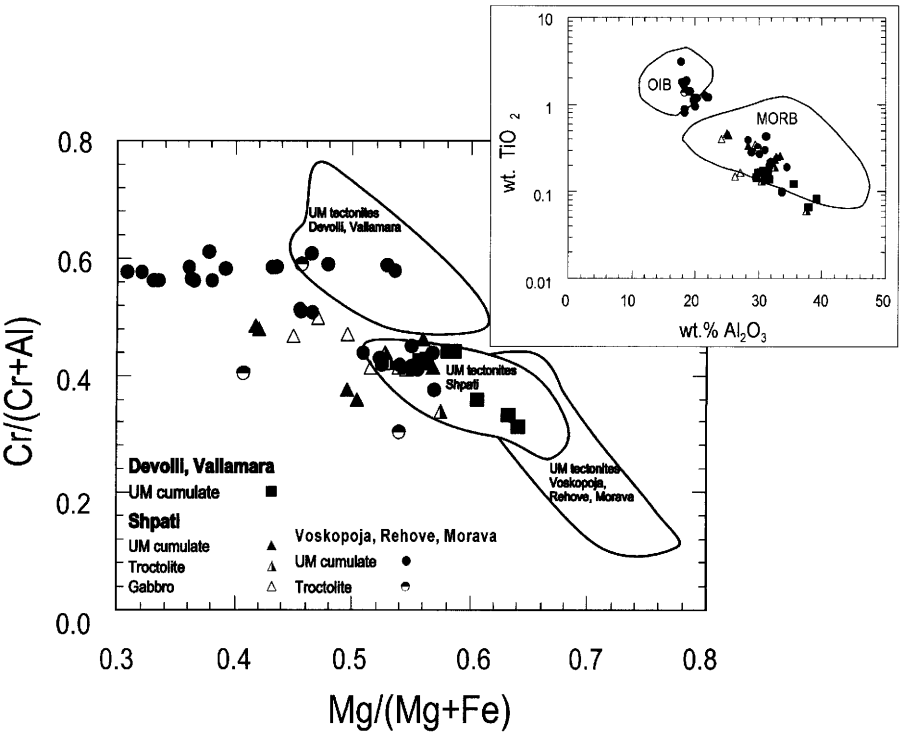

Fig. 11. X_{Mg} v. Cr-number and Al_2O_3 v. TiO_2 (inset) relations for spinel from the south Albanian ophiolites.

in the cumulates. At present, REE data exist only for the VRM ultramafic cumulates and for one from Shpati. The cumulates exhibit strongly light REE (LREE)-depleted patterns with a chondrite-normalized $(Ce/Sm)_N$ ratio of 0.3–0.4 (Fig. 16a). In contrast, the mantle tectonites, as with the lherzolites and harzburgites from VRM and DV, are enriched in the LREE relative to the middle REE (MREE); thus, they show mainly U- or spoon-shaped patterns.

Cumulate gabbros and troctolites

Analyses of cumulate gabbros are presented in Table 7. Together with the ultramafic cumulates, the cumulate gabbros and troctolites form linear arrays in the Al_2O_3 v. MgO and CaO v. MgO diagrams (Figs 13a, b and 14a, b). These arrays parallel a field between the Fo-rich olivine (Fo_{85-90}) and An-rich plagioclase (An_{80-95}). As for the ultramafic cumulates, clinopyroxene plays only a minor role in the chemical composition of the cumulate gabbros and troctolites. In general, the cumulate gabbros and troctolites are more Al_2O_3 rich (11–16 wt%) and CaO rich (8–15 wt%), but MgO poor (8–20 wt%) compared with the ultramafic cumulates. However, there is an overlap at high MgO and low Al_2O_3 and CaO contents. Na_2O is considerably higher and varies from almost 0 to 2.5 wt%; high values for K_2O (0.30 wt%) are also sometimes observed. The enrichment is probably due to sea-floor alteration. TiO_2 is, in general, below 0.35 wt%, and the X_{Mg} is variable between 0.70 and 0.86 (Fig. 15). The compatible trace elements such as Cr or Ni show significant variations up to 2000 and 1400 ppm, respectively. The incompatible trace elements contents are very low (Zr <10 ppm, Y <6 ppm, V <80 ppm). The chondrite-normalized REE patterns are generally flat, with an overall enrichment factor of 1–4; a few are slightly depleted in LREE (Fig. 16b). The pronounced positive Eu anomaly is due to plagioclase accumulation.

Isotropic gabbros and gabbronorites

Representative geochemical analyses are shown in Table 7. Gabbros and gabbronorites plot in the Al_2O_3 v. MgO diagram in a field that overlaps

Table 5. *Representative plagioclase analyses from the ultramafic cumulates (UM Cum) and all gabbroic rocks of the southern Albanian ophiolites*

Sample:	99A120	96A09	99A88	98A06	99A028	99A71	00A150	98A02	99A121B	03A362	03A350	02A319	02A280a	02A281	02A285A	02A329
Massif:	Voskopoja			Rehove					Morava	Devolli		Shpati				Luniku
Rock:	UM Cum	Gabbro	Gabbro	Gabbro	Gabbro	Troctolite	Gabbro	Gabbro	Troctolite	UM Cum	Gabbro	Plag-Dunite	Gabbro	Gabbro	Troctolite	Gabbro
SiO_2	47.69	47.11	47.24	46.41	49.14	45.73	46.67	51.88	48.99	43.99	45.91	50.95	55.00	51.34	46.14	46.72
Al_2O_3	33.14	33.58	33.20	33.65	32.01	33.62	34.13	30.23	32.07	36.23	34.61	31.00	27.69	30.11	34.60	33.47
FeO	0.27	0.00	0.55	0.41	0.41	0.38	0.49	0.30	0.13	0.06	0.04	0.16	0.24	0.60	0.03	0.43
MnO	0.03	0.00	0.00	0.00	0.00	0.01	0.04	0.01	0.01	0.00	0.00	0.01	0.02	0.00	0.05	0.03
MgO	0.00	0.00	0.09	0.03	0.19	0.04	0.10	0.01	0.00	0.00	0.02	0.01	0.00	0.13	0.00	0.03
CaO	16.42	16.59	16.97	17.58	15.47	17.96	17.68	13.16	15.15	19.17	18.17	13.96	10.91	13.99	17.82	17.34
Na_2O	2.16	2.06	2.00	1.70	2.42	1.43	1.65	4.15	3.11	0.55	1.02	3.34	5.37	3.65	1.17	1.56
K_2O	0.00	0.00	0.03	0.00	0.04	0.00	0.01	0.02	0.02	0.01	0.01	0.00	0.01	0.01	0.01	0.01
Total	99.71	99.34	100.07	99.78	99.69	99.17	100.77	99.76	99.48	100.01	99.78	99.42	99.25	99.84	99.83	99.59
Si	2.194	2.174	2.175	2.144	2.257	2.129	2.138	2.364	2.252	2.032	2.117	2.329	2.499	2.348	2.125	2.160
Al	1.797	1.826	1.801	1.833	1.733	1.844	1.843	1.623	1.737	1.973	1.881	1.670	1.483	1.622	1.878	1.823
Fe	0.011	0.000	0.021	0.016	0.016	0.015	0.019	0.012	0.005	0.002	0.002	0.006	0.009	0.023	0.001	0.017
Ca	0.809	0.821	0.837	0.870	0.761	0.896	0.868	0.642	0.746	0.949	0.898	0.684	0.531	0.685	0.879	0.859
Na	0.193	0.185	0.179	0.153	0.215	0.129	0.146	0.367	0.277	0.049	0.091	0.296	0.473	0.324	0.105	0.140
K	0.000	0.000	0.002	0.000	0.003	0.000	0.000	0.001	0.001	0.001	0.001	0.000	0.001	0.001	0.000	0.001
An	80.8	81.6	82.2	85.1	77.7	87.4	85.5	63.6	72.8	95.0	90.8	69.8	52.8	67.9	89.3	86.0

Formula calculation based on eight oxygen atoms.

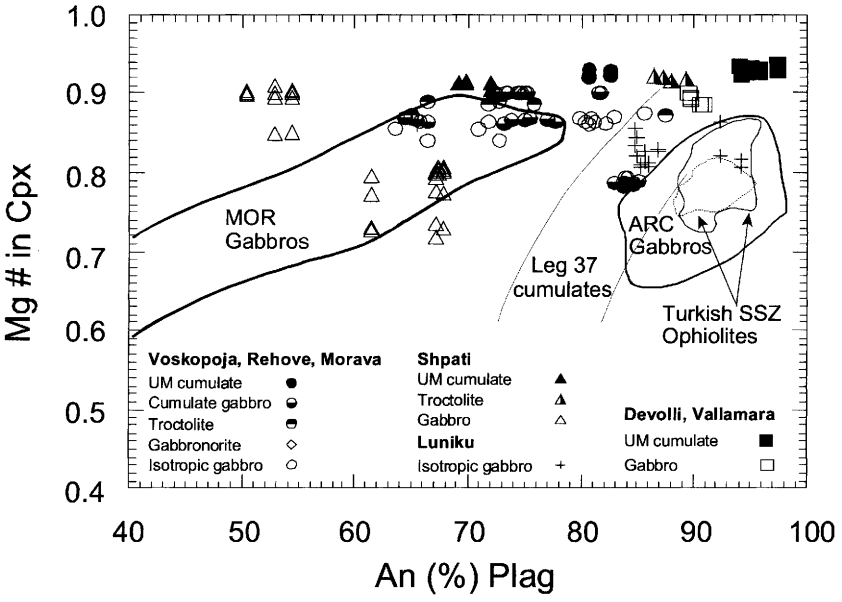

Fig. 12. An v. X_{Mg} for clinopyroxene from the south Albanian ophiolites. The field of MOR gabbros is after Ross & Elthon (1993), the field of ARC gabbros is after Burns (1985), the fields of Turkish SSZ ophiolites are after Parlak *et al.* (1996, 2000, 2002) and the Leg 37 field is after Hébert *et al.* (1989).

only to a small extent the cumulate gabbros but deviates from the cumulate array towards lower contents of MgO and Al_2O_3. This is due to the dominant role of clinopyroxene, amphibole and (partly) orthopyroxene. A similar distribution is observed in the CaO v. MgO diagram (Figs 13a, b and 14a, b).

Whereas in VRM, gabbros plot in a comparatively narrow field, the gabbros from Shpati, Devolli, Vallamara and Luniku show a much wider variation in their MgO, Al_2O_3 and CaO contents (Figs 13a, b and 14a, b). In particular, the Shpati gabbros show a high variability in CaO values; the high CaO content (up to 20 wt%) in some samples combined with low Al_2O_3 (<10 wt%) is probably due to rodingitization processes.

The compatible elements such as Cr (<1000 ppm) or Ni (<600 ppm) are relatively low in the isotropic gabbros compared with the cumulate gabbros (up to 3000 ppm Cr and 2000 ppm Ni). The content of incompatible elements is generally low, with Zr <30 ppm, Y <20 ppm and TiO_2 <0.4%. Nb is also low (1–3 ppm). In VRM and a few Shpati gabbros these elements are enriched, with Zr up to 110 ppm, Y up to 30 ppm and TiO_2 >2%. This is also valid for V, which may reach 300 ppm. The occasionally elevated values of K_2O and Na_2O are probably due to metasomatic processes during oceanic metamorphism. The REE patterns of two gabbros, one from VRM (Fig. 16a) and one from Shpati (Fig. 16b) are 10 times chondrite-enriched and display a slight upward-convex pattern. The REE patterns are not distinguishable from those of the MORB from Voskopoja or Rehove, described by Hoeck *et al.* (2002). Assuming the isotropic gabbros represent melts rather than cumulates, the most evolved gabbros match the MORB melts.

Gabbronorites are restricted to Morava, as small intrusive bodies in the cumulate gabbros. Their geochemistry falls within the range of the isotropic gabbros. They are similar to the gabbros, being high in CaO, MgO and Al_2O_3, but low in Na_2O and K_2O, and very low in TiO_2. Cr and Ni contents are in the normal range for the gabbros, but Nb, Zr and Y are extremely low.

Clinopyroxene geothermobarometry

There are a number of methods and calculations for estimating the temperatures and pressures of crystallization of basalts based on phenocryst–melt equilibria (Beattie 1993; Danyushevsky *et al.* 1996; Putirka *et al.* 1996, 2003; Yang *et al.* 1996; Métrich & Rutherford 1998; Putirka 1999). All these thermobarometers require a knowledge of the composition of the phenocrysts

Table 6. *Representative geochemical data for the ultramafic cumulate rocks of the southern Albanian ophiolites*

Sample:	A99/020	A01/226	A99/054	Alb1/98	A03/343	A03/347	A03/372	A03/353	A02/319	A03/430
Massif:	Voskopoja	Rehove			Morava	Devolli		Vallamara	Shpati	
Rock:	Plag-Per	Plag-Dunite	Wehrlite	Plag-Wehrlite	Plag-Dunite	Plag-Per	Plag-Dunite	Plag-Per	Plag-Dunite	Plag-Per
SiO_2	36.42	37.47	39.47	38.45	41.23	42.98	38.26	41.87	41.38	46.25
TiO_2	0.04	0.03	0.19	0.13	0.15	0.11	0.07	0.06	0.10	0.38
Al_2O_3	4.31	1.96	4.51	7.73	3.35	3.03	1.57	1.73	2.78	5.70
Fe_2O_3	9.00	9.69	8.77	8.41	8.28	8.96	10.15	8.28	9.13	5.98
MnO	0.12	0.09	0.13	0.12	0.12	0.13	0.14	0.12	0.13	0.12
MgO	32.89	36.38	34.71	31.45	35.41	38.64	43.25	38.79	36.97	23.11
CaO	3.85	0.10	2.50	4.02	2.67	2.73	1.04	2.05	2.31	14.34
Na_2O	0.04	0.00	0.05	0.16	0.10	0.10	0.08	0.00	0.16	0.86
K_2O	0.02	0.01	0.02	0.11	0.01	0.01	0.01	0.00	0.02	0.01
P_2O_5	0.02	0.02	0.02	0.02	0.02	0.01	0.01	0.01	0.01	0.01
LOI	13.67	13.51	9.32	9.69	8.33	3.35	4.10	6.70	6.94	3.11
Total	100.39	99.26	99.68	99.60	99.66	100.04	98.68	99.61	99.93	99.86
X_{Mg}	0.879	0.881	0.887	0.881	0.894	0.895	0.894	0.903	0.889	0.884
Nb	b.d.	0.1	0.1	b.d.	b.d.	b.d.	b.d.	b.d.	0.1	b.d.
Zr	0.6	b.d.	3.5	b.d.	7.5	1.5	1.4	0.2	5.2	11.8
Y	0.3	b.d.	3.4	2.5	2.7	2.4	b.d.	b.d.	2.5	16.4
Sr	9.7	3.4	10.0	7.6	12.4	3.4	8.0	1.6	10.9	38.0
Rb	1.2	0.1	1.0	b.d.	0.6	0.6	0.3	0.4	0.6	0.2
Ga	b.d.	3.2	b.d.	2.9	8.2	8.1	7.3	6.8	8.2	3.5
Zn	48.3	41.0	48.3	42.5	40.8	46.1	50.5	38.7	44.2	5.9
Cu	44.1	62.4	24.3	18.5	27.2	23.3	10.2	20.7	9.7	170.4
Ni	1725.7	2277.2	1940.8	1546.4	1950.5	2022.4	2370.0	2150.3	2017.9	1049.9
Co	106.5	119.3	100.4		92.4	95.0	116.9	98.9	98.0	52.8
Sc	4.0	3.1	11.0	4.9	11.8	13.6	7.1	11.3	11.1	33.3
Cr	2081.1	2633.0	3462.0	1825.8	2128.1	2397.6	2362.4	2398.9	2326.1	2374.1
V	14.2	19.2	57.1	31.9	62.8	66.6	36.0	53.7	59.2	201.1
Ba	23.5	62.4	15.0	17.8	45.3	45.6	45.1	45.6	41.2	b.d.
La			0.113	0.099					0.133	
Ce	0.022		0.337	0.411					0.480	
Pr	0.004		0.070	0.091					0.088	
Nd	0.027		0.515	0.592					0.509	
Sm	0.028		0.265	0.256					0.206	
Eu	0.027		0.129	0.126					0.090	
Gd	0.007		0.464	0.358					0.317	
Tb	0.001		0.084	0.069					0.061	
Dy	0.010		0.615	0.463					0.437	
Ho	0.004		0.138	0.100					0.100	
Er	0.008		0.437	0.304					0.312	
Tm	0.001		0.063	0.044					0.046	
Yb	0.007		0.423	0.294					0.313	
Lu	0.004		0.065	0.045					0.050	
Hf			0.177						0.847	
Ta			0.058						0.054	
Th	0.002		0.001	0.004					0.024	

REE, Hf, Ta and Th were determined by ICP-MS; all others besides LOI by XRF; Fe_{tot} as Fe_2O_3; X_{Mg} based on Fe_{tot} as FeO; b.d., below detection limit; missing values not analysed; Plag-Per, plagioclase peridotite.

as well as the composition of the liquid in equilibrium with the phenocrysts. Unfortunately, the cumulate gabbros rarely meet this requirement, as the gabbro composition does not reflect the composition of the melt in equilibrium with the crystallized phases.

The clinopyroxene barometer developed by Nimis (1995, 1999) and Nimis & Ulmer (1998)

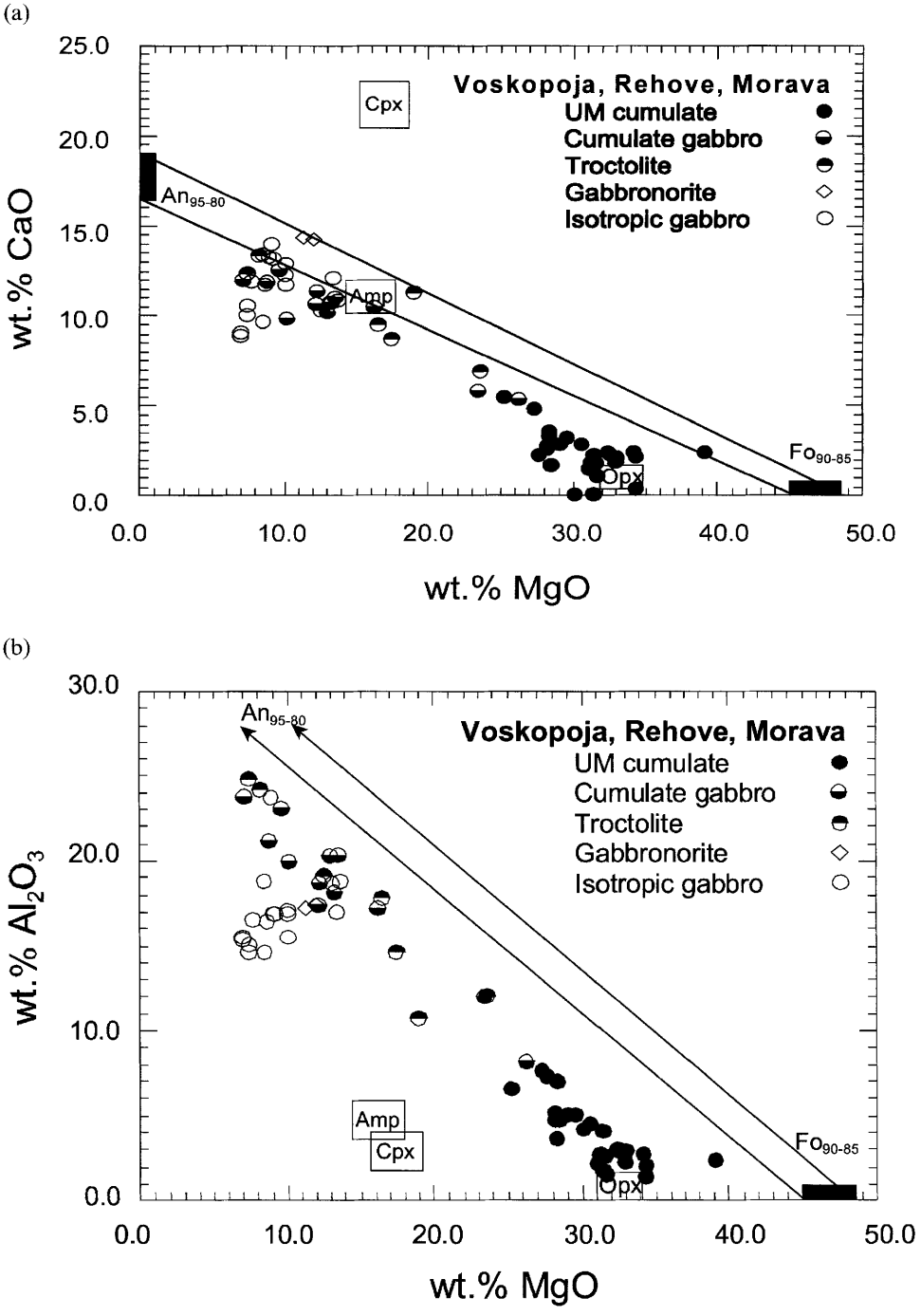

Fig. 13. (**a**) MgO v. CaO and (**b**) MgO v. Al_2O_3 for ultramafic cumulates from the Voskopoja, Rehove and Morava massifs (calculated on a dry base).

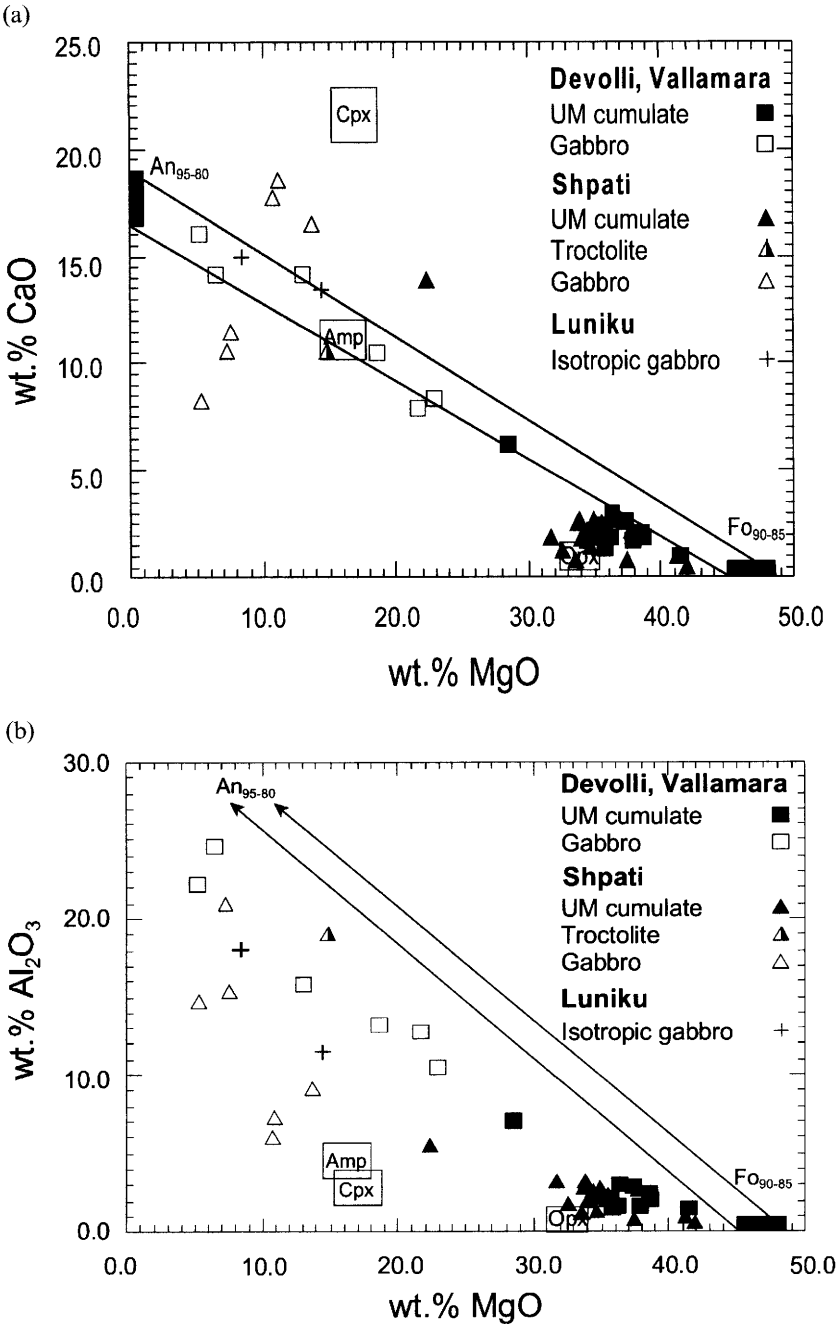

Fig. 14. (**a**) MgO v. CaO and (**b**) MgO v. Al_2O_3 for gabbros, troctolites and ultramafic cumulates from the Devolli, Vallamara, Shpati and Luniku massifs (calculated on a dry base).

approached the problem differently, utilizing structural parameters based on structural formula data for calculating the pressure. For several calculations this method requires precise temperature values with a large dependence of pressure calculations on the temperature input.

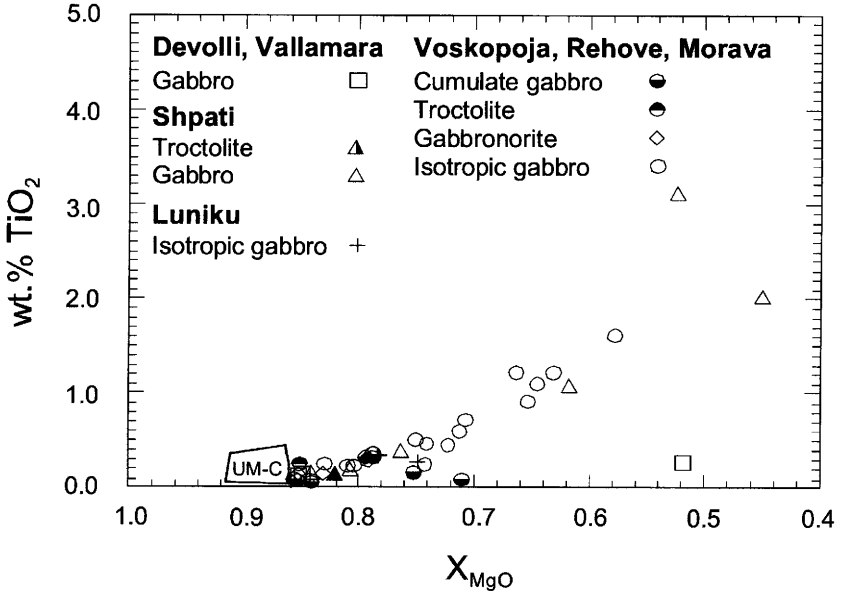

Fig. 15. X_{Mg} v. TiO_2 for ultramafic cumulates (UM-C), gabbros, troctolites and gabbronorites from the south Albanian ophiolites.

Of the four calibrations available at present for pressure calculations, only three could be applied to our samples. They cover the following compositional ranges: (1) anhydrous basic melts from basalts, through trachybasalts to low-alkali nephelinites (BA in Table 8); (2) hydrous melts of the same composition; (3) tholeiitic basalts to dacites (TH in Table 8). Calibration (1) is temperature independent and restricted to anhydrous systems; the others two can also be applied to hydrous systems but these are strongly dependent on temperature.

In the absence of reliable temperature calculations for the clinopyroxene–melt equilibrium and the rare (questionable) occurrence of magmatic hydrous phases such as magmatic amphiboles, we chose, as a first approximation, the first calibration for anhydrous quartz-normative to nepheline-normative melts. The standard error estimated by Nimis (1999) for calibration (1) is 1.7 kbar. The results are presented in Table 8 (calibration BA). It is worth mentioning that if a temperature of 1100–1150 °C is assumed, a reasonable correspondence between the pressures calculated using calibrations (1), (2) and (3) is obtained. The agreement among the three calibrations is in general better than 0.5 kbar.

However, some ultramafic, mafic cumulates and gabbros contain clinopyroxene–orthopyroxene pairs allowing temperature calculations (e.g. Brey & Köhler 1990; Taylor 1998). The application of the thermometers yielded a wide range of temperatures: 845–1070 °C (Brey & Köhler 1990) and 845–1080 °C (Taylor 1998). These temperatures are the maximum values and clearly show that subsolidus equilibration took place to a wide extent. Texturally, this is mainly expressed by clinopyroxene exsolution lamellae in orthopyroxene. The variation of Fe, Mg and Ca in clinopyroxene is relatively small.

As Nimis (1998) and later Tartarotti *et al.* (2002) pointed out, the calibration (1) by Nimis & Ulmer (1998) is independent of temperature, but underestimates the pressures for clinopyroxene recrystallized under subsolidus conditions. The pressures obtained by calibration (1) should thus be viewed as minimum values. Calibration (3) requires the temperature of crystallization. Because of the negative correlation between temperature and the calculated pressure, this calibration provides maximum values. Using temperatures calculated according to Brey & Köhler (1990) and Taylor (1998), respectively, calibration (3) results in pressures of 10–13 kbar for Morava, 9–11 kbar for Voskopoja, 9.5–11.5 kbar for Devolli and 3–9.5 kbar for the Shpati ultramafic and mafic cumulates (Table 8, calibration TH). Compared with the minimum pressure estimates (calibration BA in Table 8) for Morava, Voskopoja and Devolli the pressure brackets are large, varying from *c.* 2 kbar to a maximum of

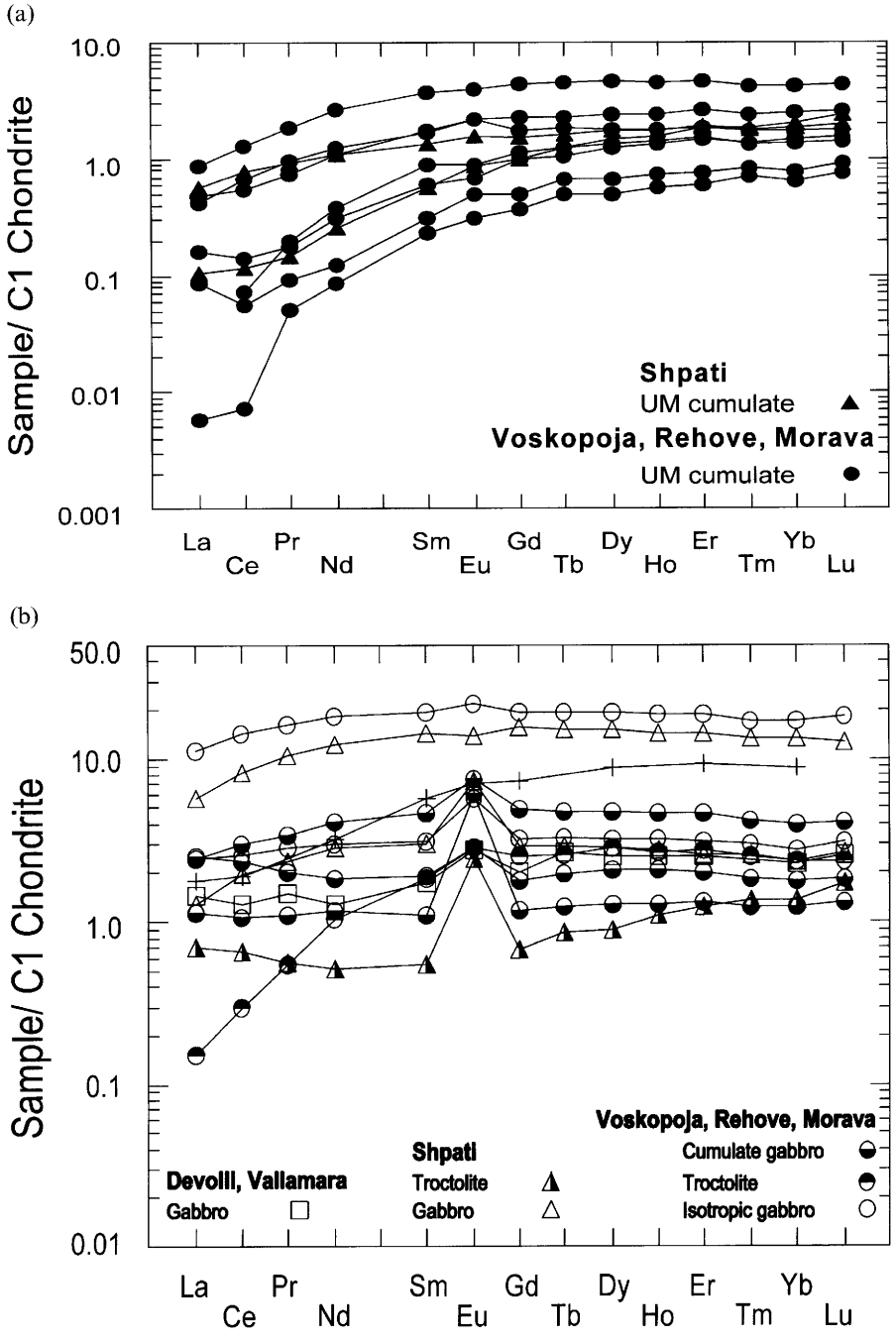

Fig. 16. (**a**) C1 chondrite-normalized REE distribution patterns for the ultramafic cumulates from the Shpati, Voskopoja, Rehove and Morava massifs. (**b**) C1 chondrite-normalized REE distribution patterns for the mafic cumulates and gabbros from (**a**) the south Albanian ophiolites.

Table 7. *Representative geochemical data for the gabbroic rocks of the southern Albanian ophiolites*

Sample:	A1010/96	A109/96	A00/139	A01/228	A99/028	Alb2/98	A99/121	A00/125
Massif:	Voskopoja			Rehove			Morava	
Rock:	Gabbro	Gabbro	Gabbro	Gabbro	Gabbro	Gabbro	Troctolite	Gabbronorite
SiO_2	39.92	43.96	50.65	37.02	46.69	48.95	42.16	50.44
TiO_2	0.05	0.09	1.62	0.14	0.33	1.21	0.15	0.14
Al_2O_3	12.88	19.09	15.14	9.07	18.06	15.01	11.48	17.60
Fe_2O_3	7.48	4.57	10.84	8.15	6.42	8.80	6.21	4.13
MnO	0.10	0.07	0.18	0.12	0.10	0.11	0.09	0.09
MgO	25.16	13.94	7.46	28.85	12.55	8.78	20.32	12.09
CaO	6.27	11.28	10.65	5.90	11.05	10.00	12.05	14.37
Na_2O	1.33	2.35	3.12	0.04	2.18	3.14	1.06	1.39
K_2O	0.02	0.02	0.28	0.01	0.11	0.56	0.04	0.10
P_2O_5	0.02	0.02	0.16	0.02	0.04	0.11	0.02	0.02
LOI	6.55	4.55	0.76	9.09	3.56	2.84	6.47	0.82
Total	99.38	99.92	100.84	98.41	101.07	99.41	100.05	101.18
X_{Mg}	0.869	0.858	0.577	0.875	0.795	0.664	0.866	0.853
Nb	b.d.	b.d.	3.2	0.1	0.6	1.3	0.1	0.8
Zr	b.d.	0.2	111.9	1.9	9.6	77.3	4.5	b.d.
Y	b.d.	0.1	31.2	1.2	3.8	26.2	1.5	1.8
Sr	25.0	679.0	172.2	6.7	133.5	191.1	479.5	89.5
Rb	b.d.	b.d.	3.4	0.6	0.8	0.0	1.3	1.1
Ga	5.0	10.0	12.9	6.6	12.3	12.2	1.0	7.5
Zn	41.0	24.0	58.7	46.9	48.5	18.1	32.7	31.2
Cu	60.0	30.0	49.8	40.7	129.3	7.8	97.7	90.5
Ni	1333.0	622.0	77.4	1699.5	494.8	104.1	926.8	329.7
Co	105.0	59.0	44.7	89.7	46.5		60.4	28.5
Sc	3.0	11.0	31.2	6.5	12.9	50.0	15.9	16.7
Cr	1775.0	793.0	190.2	8315.4	532.3	456.3	1327.0	822.1
V	20.0	33.0	220.0	71.7	79.6	231.6	59.5	98.8
Ba	b.d.	b.d.	16.1	68.7	10.0	22.1	9.6	18.5
La					0.577	2.624	0.036	
Ce		0.045			1.840	8.868	0.182	
Pr		0.008			0.325	1.533	0.052	
Nd		0.052			1.884	8.435	0.483	
Sm		0.039			0.698	2.963	0.281	
Eu		0.066			0.431	1.263	0.162	
Gd		0.064			1.022	3.923	0.511	
Tb		0.011			0.177	0.721	0.098	
Dy		0.095			1.201	4.875	0.721	
Ho		0.021			0.258	1.052	0.153	
Er		0.053			0.758	3.118	0.457	
Tm		0.004			0.109	0.443	0.063	
Yb		0.027			0.682	2.894	0.406	
Lu		0.004			0.104	0.456	0.060	
Hf					0.379		0.118	
Ta					0.100		0.025	
Th					0.017	0.124		

13 kbar. In Shpati they are smaller, at 2–9.5 kbar. For Rehove, no clinopyroxene–orthopyroxene pairs exist.

In all of the massifs the pressure brackets are wide, similar to those from the Romanche Fracture Zone (Tartarotti *et al.* 2002). Using the temperatures calculated according to Taylor (1998), the closest brackets were found in a Shpati gabbro (02A281), between 1.8 and 3.3 kbar. This indicates a depth of magma intrusion of around 5–10 km. The other brackets are not well constrained but are in accordance with such

Table 7. *Continued*

Sample:	A03/349	A03/350	A03/363	A02/280	A02/281	A02/285	A02/329	A03/444
Massif:	Devolli			Shpati			Luniku	
Rock:	Gabbro	Gabbro	Gabbro	Gabbro	Gabbro	Troctolite	Gabbro	Gabbro
SiO_2	44.64	45.17	42.24	48.34	47.76	44.61	47.83	47.90
TiO_2	0.16	0.12	0.13	2.03	1.09	0.05	0.35	0.27
Al_2O_3	16.30	13.70	10.91	15.05	15.74	19.52	11.83	18.42
Fe_2O_3	4.69	5.34	8.12	13.14	9.47	4.36	8.06	5.71
MnO	0.09	0.09	0.13	0.21	0.16	0.06	0.14	0.11
MgO	13.42	19.17	23.62	5.42	7.76	15.20	14.76	8.59
CaO	14.57	10.82	8.61	8.45	11.70	10.90	13.80	15.26
Na_2O	3.01	2.43	2.09	4.33	2.81	2.66	0.74	1.65
K_2O	0.02	0.02	0.05	0.30	0.13	0.01	0.02	0.13
P_2O_5	0.01	0.01	0.01	0.15	0.07	0.01	0.02	0.01
LOI	3.07	3.13	3.14	2.19	2.16	2.59	2.64	2.17
Total	99.97	99.99	99.04	99.62	98.83	99.97	100.18	100.23
X_{Mg}	0.850	0.877	0.852	0.449	0.619	0.873	0.784	0.749
Nb	b.d.	b.d.	0.1	b.d.	b.d.	b.d.	0.4	2.4
Zr	1.1	2.2	2.9	103.2	48.5	1.4	9.4	13.8
Y	6.6	4.0	2.6	48.6	29.4	5.9	16.9	9.3
Sr	44.8	54.0	71.3	155.3	122.3	92.3	39.5	48.8
Rb	1.0	0.7	1.0	2.3	1.2	b.d.	b.d.	4.9
Ga	14.4	12.5	12.2	26.6	24.2	14.2	15.9	13.5
Zn	25.9	32.8	43.7	89.5	65.4	27.6	46.8	22.6
Cu	23.7	55.4	64.8	38.4	69.8	49.7	133.6	93.3
Ni	420.4	933.6	1152.6	49.6	128.6	661.7	347.8	147.2
Co	36.1	45.8	69.0	42.0	39.1	36.2	49.5	19.6
Sc	37.1	20.3	14.4	32.5	30.9	12.0	34.1	17.1
Cr	1006.6	1753.7	2721.7	79.4	355.2	654.1	1135.7	538.6
V	170.8	90.8	69.9	305.4	223.2	35.4	178.5	141.8
Ba	43.0	43.9	45.3	b.d.	b.d.	6.8	b.d.	30.5
La			0.346	1.369		0.163	0.429	
Ce			0.795	5.013		0.407	1.168	
Pr			0.141	0.985		0.054		
Nd			0.604	5.689		0.239	1.486	
Sm			0.268	2.214		0.084	0.868	
Eu			0.162	0.811		0.140	0.417	
Gd			0.421	3.231		0.137	1.493	
Tb			0.100	0.564		0.032		
Dy			0.629	3.807		0.229	2.221	
Ho			0.144	0.800		0.063		
Er			0.420	2.373		0.204	1.541	
Tm				0.342		0.035		
Yb			0.388	2.256		0.230	1.477	
Lu			0.066	0.325		0.044		
Hf			0.032			0.768	0.242	
Ta			0.290			0.226	0.654	
Th			0.282	0.065		0.146	0.303	

REE, Hf, Ta and Th were determined by ICP-MS; all others besides LOI by XRF; Fe_{tot} as Fe_2O_3; X_{Mg} based on Fe_{tot} as FeO; b.d., below detection limit; missing values not analysed.

an intrusion depth. In Shpati and Devolli, there are no volcanic or plutonic rocks superimposed on the thin gabbro sequence to account for the depth of the gabbro intrusions. The original overburden was presumably tectonically eroded, possibly creating 'turtleback' domes by mantle denudation (Tucholke *et al.* 1998; Nicolas *et al.* 1999).

Table 8. *Clinopyroxene geothermobarometry and clinopyroxene–orthopyroxene thermometry*

Rock	Sample	P (kbar) Cal. BA	T (°C) Taylor	P (kbar) Cal. TH	T (°C) Brey & Köhler	P (kbar) Cal. TH
Voskopoja						
Gabbro	02A323	1.8				
Plag-Peridotite	99A020	2.4	925	<10.9	981	<8.9
Rehove						
Gabbro	98A05	1.8				
Gabbro	99A028	4.1				
Wehrlite	99A028	2.1				
Plag-Peridotite	99A054	2.8				
Morava						
Troctolite	99A121B	1.5				
Plag-Dunite	99A088	3.1	867	<13.0	928	<10.8
Plag-Peridotite	99A120	2.4	884	<11.3	931	<9.7
Devolli						
Gabbro	03A350	2.2	940	<9.5	919	<10.3
Plag-Peridotite	03A362	1.6	843	<11.5	846	<11.4
Shpati						
Troctolite	2A285a	1.4	1033	<4.7	959	<7.5
Gabbro	02A281	1.8	1067	<3.2	983	<6.6
Gabbro	02A280	3.8	1032	<8.4	1050	<7.4
Plag-Dunite	02A323	2.2	922	<9.6	956	<8.3
Plag-Dunite	02A319	3.1	1011	<7.9	1079	<5.3
Luniku						
Gabbro	02A329	1.9				

Clinopyroxene geothermobarometry according to Nimis (1995, 1999) and Nimis & Ulmer (1998). Clinopyroxene–orthopyroxene thermometry after Brey & Köhler (1990) and Taylor (1998). Pressure calibrations: Cal. BA, anhydrous basalt, Cal. TH, tholeiitic basalt.

Discussion

MOR v. SSZ origin: geochemical and mineral-chemical evidence

During the last 25 years a number of attempts have been made to solve a longstanding controversy concerning the interpretation of ophiolites, the so-called 'ophiolite conundrum' (Moores *et al.* 2000): did they form in a mid-oceanic ridge environment, which is documented by their structure, or in a marginal basin (SSZ), which is indicated by their geochemistry? Extensive reviews of this problem were recently published by Hawkins (2003) and Pearce (2003).

Apart from the geological evidence, the whole-rock geochemistry, in particular the immobile trace elements, the mineral chemistry, and the petrological and isotopic evidence have been used to discriminate between MOR and SSZ environments (Pearce 2003). Many of the discrimination methods apply only to unaltered rocks and uncontaminated basalts. Whereas lavas are often severely altered, impeding geochemical discrimination, gabbros are often less altered but are affected by cumulus and assimilation processes or trapped melts. Nevertheless, some gabbros can be discriminated on their whole-rock geochemistry (Serri 1981).

The incompatible elements are low in some gabbros, but a number of isotropic gabbros from Morava, Rehove and Voskopoja, as well as some from Shpati, have higher values in the range of MORB. The former show a very low mafic index (M.I. <0.3), as defined by Serri (1981), where a discrimination of high- or low-Ti gabbros is not feasible; the latter classify as high-Ti gabbros (Serri 1981). Zr/Y ratio is 3–4 and the V/Ti × 1000 ratio is >20 for most of the isotropic gabbros from VRM and for some from Shpati. Other isotropic gabbros such as those from Devolli, Luniku and some from Shpati show much lower values: Zr/Y <2 and V/Ti <20. Provided the former gabbros represent true melts with no cumulate components, they can be interpreted as being derived from MOR-type magmas. This is corroborated by a rock/MORB plot, which shows a flat pattern clustering around unity for the isotropic gabbros from VRM (Fig. 17a) and by the REE pattern (Fig. 16b). Conversely, many gabbros from Shpati (except one sample with MOR characteristics), and those from Luniku and Devolli show a marked depletion of HFSE (Nb to Y; Fig. 17b),

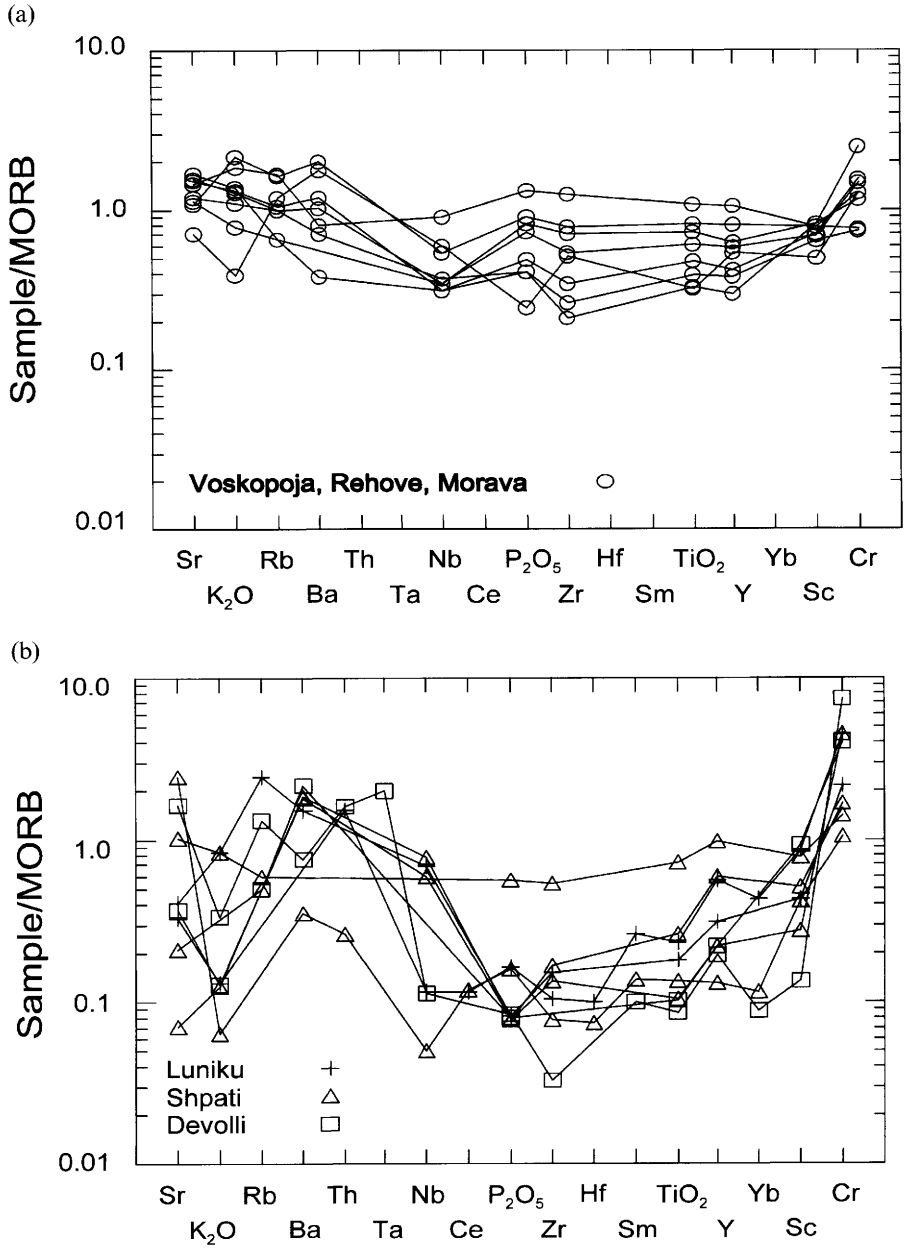

Fig. 17. (**a**) Spider diagrams of MORB-normalized trace element abundances in the isotropic gabbros from the Voskopoja, Rehove and Morava massifs. (**b**) the Luniku, Shpati and Devolli massifs.

consistent with their formation in an SSZ environment. The variability in LILE is due to low-temperature alteration. Gabbros from Devolli, Luniku and most of them from Shpati represent SSZ-type magmas.

A number of the compositional ranges of the most important minerals in cumulates, such as clinopyroxene, orthopyroxene, spinel or plagioclase, have been used to distinguish between MOR-related and subduction-related cumulates and gabbros. In particular, the An content of plagioclase is used commonly in connection with X_{Mg} in clinopyroxene (Fig. 12) or forsterite content in olivine (Fig. 8) to discriminate between MOR

and arc gabbros (Burns 1985; Beard & Borgia 1989; Parlak *et al.* 1996, 2000). In Figure 12, the MOR field was taken from Burns (1985), Ross & Elthon (1993) and Schmincke *et al.* (1998), the Leg 37 field from Hébert *et al.* 1989), and the arc field from Burns (1985), including the field of Turkish ophiolites from Parlak *et al.* (1996, 2000). The cumulates and gabbros show a wide range in An content (only An-rich cores were used) from 50 to 97 and a smaller spread in X_{Mg} clinopyroxene from 0.70 to 0.97. High X_{Mg} has been noted by Elthon *et al.* (1982, 1992) and by Komor *et al.* (1985) for gabbros from the Bay of Islands and from oceanic gabbros, and was interpreted as an indication of moderate- to high-pressure crystallization of the gabbros in an island arc environment. However, Bédard & Hébert (1996, 1998) showed that the high X_{Mg} in clinopyroxene is due to reaction–assimilation processes unrelated to high pressure.

Most troctolites and isotropic gabbros from VRM, and some ultramafic cumulates and isotropic gabbros from Shpati, indicate a MOR composition. Ultramafic cumulates and gabbros from DV, isotropic gabbros from Luniku and a few cumulate gabbros from VRM plot in the area close to the arc gabbros field. Ultramafic cumulates from VRM, a few gabbros from VRM, and troctolites from Shpati with high An and X_{Mg} plot between the two fields. In particular, gabbros from Luniku and a few cumulate gabbros from VRM overlap with the Leg 37 field from the Central Atlantic.

Gabbros with high-An plagioclase and X_{Mg} clinopyroxene described by Ross & Elthon (1993), from Site 334 west of the Mid-Atlantic Ridge, are also from Leg 37. Their Na_2O and TiO_2 contents in clinopyroxene are as low as in those from DV and Luniku. Ross & Elthon (1993) concluded that these depleted clinopyroxenes formed in a MOR environment from a strongly depleted liquid, which was then collected in a crustal magma chamber to form cumulates. Eventually, the cumulates interacted with more enriched liquids migrating through them by porous flow.

In a similar way, the Cr-number in spinels is indicative of the environment of formation, as the MOR-type spinels have, in general, Cr-number below 0.50, and spinels from the subduction-related gabbros and cumulates have Cr-number around 0.60 and higher (Dick & Bullen 1984; Allan *et al.* 1988; Hébert *et al.* 1989). In the Cr-number v. Mg-number diagram (Fig. 11), the VRM mantle tectonites plot in the field of ocean-floor peridotites (peridotites I of Dick & Bullen 1984), whereas the DV harzburgites in the peridotite III field and the Shpati ultramafic rocks have an intermediate position. Spinels of ultramafic and mafic cumulates show a Cr-number of 0.3–0.6 and a Mg-number of 0.3–0.64. The variability in the Mg-number of VRM ultramafic cumulates at Cr-number around 0.6 is possibly due to subsolidus re-equilibration (Roeder 1994). Kamenetsky *et al.* (2001) presented a new discrimination diagram based on TiO_2 and Al_2O_3 contents in spinel. They argued that other than Mg-number and Cr-number, TiO_2 and Al_2O_3 reflect the melt composition and are thus potential discriminating elements for the tectonic setting of spinel-bearing magmas.

The comparison of spinels from olivine-bearing cumulates in terms of Ti and Al are shown in the inset in Figure 11. There is a clear negative correlation of TiO_2 with Al_2O_3. Two groups can be distinguished; the larger one is compatible with a MOR environment; the second is enriched in TiO_2 and partially overlaps with the ocean island basalt (OIB) field (consisting in large part of the ultramafic cumulates from VRM). It should be noted that spinels of the ultramafic rocks from DV are high in Al_2O_3 and plot in the MOR field, suggesting that at least the spinels came from a magma with a MOR affinity, whereas other parameters such as high An, Fo and X_{Mg} in clinopyroxene suggest an SSZ affinity.

Olivine is mainly confined to the ultramafic cumulates, troctolites and cumulate gabbros but is rare in the isotropic gabbros. The forsterite content is limited to between Fo_{82} and Fo_{90}. When combined with the An content of plagioclase (Fig. 8), almost all of the olivines plot in the field of oceanic cumulates, as defined by Beard (1986). Only few plagioclase–olivine pairs, with high An content and a lower Fo content, plot outside, in the field delineated for the Oman gabbros by Browning (1984) and closer to the arc gabbros and the field of the Turkish and Troodos gabbros, respectively (Elthon 1987; Parlak *et al.* 2000, 2002). Again, as with the X_{Mg} clinopyroxene v. An diagram, the anorthite component would be consistent with arc gabbros but the Mg-number of clinopyroxene as well as the Fo content are too high to fit well into the delineated field of arc gabbros. The high X_{Mg} of clinopyroxene, orthopyroxene and probably olivine is interpreted as an indicator of magma crystallization at moderate pressures (Elthon *et al.* 1982; Elthon 1987; Parlak *et al.* 1996, 2000, 2002).

The composition of clinopyroxene in terms of Ti, Mg, Mn, Si and Al is used widely to discriminate pyroxenes from various environments. All of the diagrams, such as TiO_2–Na_2O–MnO (Nisbet & Pearce 1977), TiO_2–Na_2O–$SiO_2/100$,

Na v. Ti or Al^{IV} v. Ti (Beccaluva *et al.* 1989), Al^{IV} v. Ti (Loucks 1990), or Ti + Cr v. Ca (Leterrier *et al.* 1982) exhibit a considerable overlap between clinopyroxene compositions formed in a MOR environment and those formed in an intraplate or SSZ environment. The discrimination is mainly based on the Ti/Na and the Ti/Al^{IV} ratios. Clinopyroxenes from cumulates and gabbros show a wide variation of all ratios. Clinopyroxenes of most cumulate gabbros and some ultramafic cumulates show a Ti/Na ratio <0.4 and Ti/Al^{IV} ratio <0.15, as do those from the ultramafic cumulates, troctolites and some gabbros from Shpati. The low ratios are even more pronounced for the Devolli and Vallamara ultramafic cumulates and gabbros and are also observed in same isotropic gabbros from Luniku. The high Ti/Na (>0.4) and Ti/Al^{IV} (>0.15) ratios are found in most ultramafic cumulates from VRM (high-Ti clinopyroxenes) in most of the Shpati gabbros, and in some Luniku isotropic gabbros. Most isotropic gabbros from VRM have an intermediate ratio between the two groups.

The first group represents those cumulates and gabbros with high X_{Mg} in clinopyroxene and high An in plagioclase, which plot in Figure 12 outside the field of MOR gabbros and close to, or inside, the arc gabbros field. All of these features, the high X_{Mg} in clinopyroxene, the high An content in plagioclase, and the low Ti/Na and Ti/Al^{IV} ratio in clinopyroxenes, indicate that these cumulates and gabbros did not form in a MOR environment, but crystallized instead from primitive high-MgO and low-TiO_2 melts in an environment related to a subduction zone. The second Ti-rich group has more in common with typical MOR magmas, i.e. high Ti and Na contents in clinopyroxenes, partly lower X_{Mg} in clinopyroxenes and a lower An content in plagioclase. It should be noticed, however, that both magma groups do not form distinct fields but rather show a gradation in composition.

Summarizing, the ultramafic and mafic cumulates and isotropic gabbros show a wide variety of geochemical compositions of the whole rock as well as of the minerals such as olivine, plagioclase, clinopyroxene and spinel. In various discrimination diagrams they form continuous arrays, ranging in many cases from the MOR to SSZ fields. The most discriminating elements or element ratios are consistent as they show MOR and SSZ environments for the same groups of rocks. Peridotites are predominantly lherzolitic for VRM, harzburgitic for DV, and show lherzolitic and harzburgitic composition for Shpati. This is also reflected in the spinel composition of the mantle tectonites in Figure 11. Based on X_{Mg} in clinopyroxene and the anorthite in plagioclase relationship (Fig. 12), most of the VRM cumulate gabbros and troctolites, as well as some isotropic gabbros from VRM and Shpati, and the Shpati ultramafic cumulate are consistent with a MOR origin. On the other hand, the DV ultramafic cumulate, gabbros, some isotropic gabbros from Luniku and troctolites from Shpati indicate an SSZ environment, whereas ultramafic cumulates and some gabbros of VRM are intermediate. Where olivines are preserved in the SSZ group, they plot on the An v. Fo diagram in the 'Oman' field (Browning 1984).

The composition of clinopyroxene shows the same pattern. The low Ti content in some ultramafic to mafic cumulates and a few isotropic gabbros suggests an SSZ origin, similar to troctolites and some gabbros from Shpati, and some Luniku gabbros and ultramafic cumulates and gabbros from DV. Despite a relatively wide range of overlap, it is clear that a number of gabbros were most probably generated in an SSZ environment.

Tectonic setting

Any discussion on the tectonic setting of the Albanian ophiolites has to take into account that the Albanian ophiolites are only a small fraction of a much larger belt extending between Croatia and Greece. Unfortunately, the Dinaric ophiolites are not very well investigated. More modern studies exist only for the northern part (Pamić *et al.* 2002, and references herein). In Greece, the neighbouring ophiolites, Pindos and Vourinos, are much better investigated. (For recent reviews see Smith & Rassios (2003); Bortolotti *et al.* (2004) and Rassios & Moores (2006).

Until a few years ago, the Albanian ophiolites were seen as a MORB-like western belt and an SSZ-like eastern belt. This view came from the structure of the ophiolites (Shallo 1992, 1994; Robertson & Shallo 2000; Shallo & Dilek 2003) and was supported by some petrological and geochemical studies (Beccaluva *et al.* 1994*b*; Bortolotti *et al.* 1996). All of the tectonic models focused on a duality involving a normal mid-ocean spreading to create a MOR-type ocean crust, to which SSZ-type crust was added later above an intra-oceanic subduction zone.

In the Pindos ophiolite, which can be considered as the continuation of the western MOR-type ophiolite in Albania, geochemical analysis (Capedri *et al.* 1980; Pearce *et al.* 1984; Jones

et al. 1991; Smith & Rassios 2003; Saccani & Photiades 2004) revealed, besides a MORB character, an SSZ contribution in the lavas and dykes. Hoeck & Koller (1999) showed for the first time that in the western ophiolite belt in southern Albania, SSZ lavas also occur. Later Bortolotti *et al.* (2002) and Hoeck *et al.* (2002) reported a wider occurrence of SSZ lavas from the southern and northern parts of the western ophiolite belt, demonstrating that the western belt also shows at least some subduction influence. This is supported by the present study.

An SSZ signature has been reported from cumulates and basalts from a mid-ocean environment (west of Mid-Atlantic Ridge, and the Chile Ridge adjacent to the Chile Trench) (Ross & Elthon 1993; Klein & Karsten 1995; Sturm *et al.* 2000). The close proximity of the western belt to the arc-related magmas (eastern belt, Pindos), combined with a relatively thick cover of volcaniclastic sediments and turbidites, makes it likely that it was generated in an SZZ environment; nevertheless, MOR-type lavas prevail.

Whether the western belt formed in a fore-arc setting (Bortolotti *et al.* 2002) or a back-arc setting (Hoeck *et al.* 2002) is difficult to assess. The SSZ magma was erupted or intruded relatively late as the dykes and gabbros intrude earlier MOR magma-derived cumulates. In part, both lava types erupted simultaneously (Bortolotti *et al.* 2002). From this relationship and the late occurrence of (rare) boninites, Bortolotti *et al.* (2002) inferred a fore-arc setting above an eastward-directed subduction zone. On the other hand, the predominance of MOR magma is consistent with a back-arc basin (see Smith & Rassios 2003; Saccani *et al.* 2004), in which MOR lavas and island arc-related magmas may erupt simultaneously (e.g. Mariana back-arc basin, Hawkins 2003).

In addition to a fore-arc spreading setting, Deschamps & Lallemand (2003) pointed out that boninites could occur within back-arc spreading centres if (1) a spreading centre propagates at a low angle to the associated volcanic arc, (2) a spreading centre intersects a transition between a subduction zone and a transform fault at a high angle or (3) a spreading centre intersects a transform fault at right angles, and this subsequently changes into an incipient subduction zone (see also Monzier *et al.* 1993).

An example of scenario (1) is the Valu Fa ridge, which is at a very low angle to the Tofua arc (Kamenetsky *et al.* 1997), and an example of scenario (2) is the southern Andaman Sea (Moores *et al.* 1984; Harris 2003). Both basins may serve as a model for the Albanian ophiolites. The strongly depleted DV massifs with their most pronounced arc signature are difficult to interpret. If they were originally situated within the western belt, they could be viewed as possible older rifted arc crust, which was later segmented into ridges and troughs, as reported by Parson & Hawkins (1994) for the western part of the Lau basin. Alternatively, they could be thrust westwards from an original position further east between the Shebeniku and Bilisht massifs, to their present position between Voskopoja and Shpati. However, this needs to be tested further by structural studies along the boundaries of both massifs.

Our findings and even the occurrence of some boninites (Bortolotti *et al.* 2002) do not contradict an origin of the western ophiolites in a back-arc basin. However, the interpretation of the western ophiolite belt as a fore-arc or back-arc basin has some implications for the direction of subduction. If the western belt represents a fore-arc and the eastern belt an incipient arc, an eastward-dipping subduction zone relative to the present coordinates is more probable. If the western belt formed in a back-arc, a model we favour, a west-dipping subduction zone is more probable (see also Saccani *et al.* 2004).

Despite a wealth of petrological and geochemical data from the ophiolites of Albania and Greece, more systematic petrological–geochemical mapping along and across the ophiolite belts is still needed to elucidate their mutual relationship. Additionally, the sediments on top of the ophiolites and the denudation of the ultramafic massifs of Devolli, Vallamara, Morava and Shpati deserve detailed investigations to resolve the problems of genesis of the Albanide–Dinaride ophiolites.

Conclusions

(1) The southern Albanian ophiolites consist of a number of individual bodies, each with a distinct geology and lithology. They comprise lherzolites, plutonic rocks and mainly basaltic volcanic rocks in Voskopoja and Rehove, units with lherzolites–harzburgites and plutonic rocks in Morava and Shpati, and massifs with only harzburgites and a thin plutonic cap in Devolli and Vallamara.

(2) The plutonic sequence contains ultramafic cumulates (e.g. plagioclase-bearing dunites, wehrlites), cumulate gabbros, troctolites and isotropic clinopyroxene gabbros. Gabbronorites are rare. The whole-rock geochemistry of the isotropic gabbros and the

mineralogy of all of the cumulate rocks such as X_{Mg} of clinopyroxene, An content of plagioclase, forsterite content in olivine and spinel chemistry indicate a wide compositional field for gabbros, ranging from MOR- to SSZ-type rocks.

(3) Cumulates and gabbros from Voskopoja, Rehove and Morava predominantly show a MOR composition with a minor SSZ fingerprint, whereas mantle tectonites and cumulates from Devolli and Vallamara almost exclusively exhibit an SSZ signature. In Shpati and the small Luniku massif SSZ plutonic rocks occur together with a considerable amount of MOR-type gabbros. Our findings show that in the western ophiolite belt of southern Albania a considerable amount of SSZ magmas occur, not only within the volcanic rocks (Bortolotti *et al.* 2002; Hoeck *et al.* 2002) but also in the plutonic rocks.

(4) The predominance of MOR-type over SSZ-type crustal rocks together with the occurrence of volcanogenic sediments on top of the ophiolites support an origin of the ophiolites in a back-arc basin. The harzburgitic bodies from Devolli and Vallamara, as well as the occasional occurrence of boninites, do not exclude a back-arc basin formation. This contrasts with an alternative view by Bortolotti *et al.* (2002), in which the western belt ophiolites formed in a fore-arc basin. The interpretation of the western ophiolite belt as back-arc or as fore-arc derived has some implications for the direction of the subduction. In the first case, a westward-dipping subduction is indicated; in the second, the subduction should dip to the east.

This research was substantially supported by the Austrian Nationalbank (Jubiläumsfond) Project No. 7602 and by the Albanian Geological Survey in Tirana. The branch in Korce was helpful with logistic support. We would like to thank also in particular F. Dafa, K. Gjata, H. Hallaci, E. Bedini, M. Besku and last but not least S. Bushati (all Tirana), as well as H. Pula and P. Kalina (Korce), for an introduction to the geology of Albania and the Albanian ophiolites. The microprobe measurements were carried out by D. Topa (University of Salzburg). The XRF analyst was P. Nagl (University of Vienna). Finally, we would also like to thank the Austrian Embassy in Tirana, and the ÖAD for the continual support of our research work. The manuscript benefited substantially from the careful reviews by P. Nimis and R. Hébert. Their comments improved our thinking on petrological problems in ophiolites. Special thanks go to A. H. F. Robertson, one of the editors of this volume, for his thoughtful review and his continuous support and help.

References

ALLAN, J. F., SACK, R. & BATIZA, R. 1988. Cr-rich spinels as petrogenetic indicators: MORB-type lavas from the Lamont seamount chain, eastern Pacific. *American Mineralogist*, **73**, 741–753.

BEARD, J. S. 1986. Characteristic mineralogy of arc-related cumulate gabbros: implications for the tectonic setting of gabbroic plutons and for andesite genesis. *Geology*, **14**, 848–851.

BEARD, J. S. & BORGIA, A. 1989. Temporal variation of mineralogy and petrology in cognate gabbroic enclaves at Arenal volcano, Costa Rica. *Contributions to Mineralogy and Petrology*, **103**, 110–122.

BEATTIE, P. 1993. Olivine–melt and orthopyroxene–melt equilibria. *Contributions to Mineralogy and Petrology*, **115**, 103–111.

BECCALUVA, L., MACCIOTTA, G., PICCARDO, G. B. & ZEDA, O. 1989. Clinopyroxene composition of ophiolite basalts as petrogenetic indicator. *Chemical Geology*, **77**, 165–182.

BECCALUVA, L., COLTORTI, M., DEDA, T., *et al.* 1994*a*. A cross section through western and eastern ophiolitic belts of Albania (Working Group Meeting of IGCP Project 256—Field Trip A). *Ofioliti*, **19**(1), 3–26.

BECCALUVA, L., COLTORTI, M., PREMTI, I., SACCANI, E., SIENA, F. & ZEDA, O. 1994*b*. Mid-ocean ridge and suprasubduction affinities in the ophiolitic belts of Albania. *Ofioliti*, **19**(1), 77–96.

BÉDARD, J. H. & HÉBERT, R. 1996. The lower crust of the Bay of Island ophiolite, Canada: petrology, mineralogy, and the importance of syntexis in magmatic differentiation in ophiolites and at ocean ridges. *Journal of Geophysical Research*, **103**(B3), 5165–5184.

BÉDARD, J. H. & HÉBERT, R. 1998. Formation of chromitites by assimilation of crustal pyroxenites and gabbros into peridotidic intrusions: North Arm Mountain massif, Bay of Islands ophiolite, Newfoundland, Canada. *Journal of Geophysical Research*, **101**(B11), 25105–25124.

BORTOLOTTI, V., KODRA, A., MARRONI, M., MUSTAFA, F., PANDOLFI, L., PRINCIPI, G. & SACCANI, E. 1996. Geology and petrology of ophiolitic sequences in the Mirdita region (northern Albania). *Ofioliti*, **21**(1), 3–20.

BORTOLOTTI, V., MARRONI, M., PANDOLFI, L., PRINCIPI, G. & SACCANI, E. 2002. Interaction between mid-ocean ridge and subduction magmatism in Albanian ophiolites. *Journal of Geology*, **110**, 561–576.

BORTOLOTTI, V., CHIARI, M., MARCUCCI, M., MARRONI, M., PANDOLFI, L. & PRINCIPI, G. 2004. Comparison among the Albanian and Greek ophiolites: in search of constraints for the evolution of the Mesozoic Tethys Ocean. *Ofioliti*, **29**(1), 19–35.

BREY, G. P. & KÖHLER, T. 1990. Geothermometry in four-phase lherzolites II. *Journal of Petrology*, **31**, 1353–1378.

BROWNING, P. 1984. Cryptic variation within the cumulate sequence of the Oman ophiolite: magma chamber depth and petrological implications.

In: GASS, G. I., LIPPARD, S. J. & SHELTON, A. W. (eds) *Ophiolites and Oceanic Lithosphere*. Geological Society, London, Special Publications, **13**, 71–82.

BURNS, L. E. 1985. The Border Ranges ultramafic and mafic complex, south–central Alaska: cumulate fractionates of island-arc volcanics. *Canadian Journal of Earth Sciences*, **22**, 1020–1038.

CAPEDRI, S., VENTURELLI, G., BOCCHI, G., DOSTAL, J., GARUTI, G. & ROSSI, A. 1980. The geochemistry and petrogenesis of an ophiolitic sequence from Pindos, Greece. *Contributions to Mineralogy and Petrology*, **74**, 189–200.

CORTESOGNO, L., GAGGERO, L., JAHO, E., MARRONI, M., PANDOLFI, L. & SHTJEFANAKU, D. 1998. The gabbroic complex of the western ophiolitic belt, Northern Albania: an example of multilayered sequence in an intermediate-spreading oceanic ridge. *Ofioliti*, **23**(2), 49–64.

DANYUSHEVSKY, L. V., SOBOLEV, A. V. & DMITRIEV, L. V. 1996. Estimation of the pressure of crystallization and H_2O content of MORB and BABB glasses: calibration of an empirical technique. *Mineralogy and Petrology*, **57**, 185–204.

DESCHAMPS, A. & LALLEMAND, S. 2003. Geodynamic setting of Izu–Bonin–Mariana boninites. *In*: LARTER, R. D. & LEAT, P. T. (eds) *Intra-oceanic Subduction System: Tectonic and Magmatic Processes*. Geological Society, London, Special Publications, **219**, 163–185.

DICK, H. J. B. & BULLEN, T. 1984. Chromium spinel as petrogenetic indicator in abyssal and alpine-type peridotites, and spatially associated lavas. *Contributions to Mineralogy and Petrology*, **86**, 54–76.

DILEK, Y., SHALLO, M. & FURNES, H. 2005. Rift–drift, seafloor spreading, and subduction tectonics of Albanian ophiolites. *International Geology Review*, **47**, 147–176.

ELTHON, D. 1987. Petrology of gabbroic rocks from the Mid-Cayman Rise spreading center. *Journal of Geophysical Research*, **92**(B1), 658–682.

ELTHON, D., CASEY, J. F. & KOMOR, S. 1982. Mineral chemistry of ultramafic cumulates from the North Arm Mountain Massif of the Bay of Islands ophiolite: evidence for high-pressure crystal fractionation of oceanic basalts. *Journal of Geophysical Research*, **87**(B10), 8717–8734.

ELTHON, D., STEWART, M. & ROSS, K. 1992. Compositional trends of minerals in oceanic cumulates. *Journal of Geophysical Research*, **97**(B11), 15189–15199.

FRASHERI, A., NISHANI, P., BUSHATI, S. & HYSENI, A. 1996. Relationship between tectonic zones of the Albanides, based on results of geophysical studies. *In*: ZIEGLER, P. A. & HORWATH, F. (eds) *Peri-Tethys Memoir 2: Structure and Prospects of Alpine Basins and Forelands*. Mémoires du Múseum National d'Histoire Naturelle, **170**, 485–511.

HARRIS, R. 2003. Geodynamic patterns of ophiolites and marginal basins in the Indonesian and New Guinea regions. *In*: DILEK, Y. & ROBINSON, P. T. (eds) *Ophiolites in Earth History*. Geological Society, London, Special Publications, **218**, 481–505.

HAWKINS, J. W. 2003. Geology of supra-subduction zones—implications for the origin of ophiolites. *In*: DILEK, Y. & NEWCOMB, S. (eds) *Ophiolite Concept and the Evolution of Geological Thought*. Geological Society of America, Special Papers, **373**, 227–268.

HÉBERT, R. & LAURENT, R. 1990. Mineral chemistry of the plutonic section of the Troodos ophiolite: new constraints for genesis of arc-related ophiolites. *In*: MALPAS, J., MOORES, E. M., PANAYIOTOU, A. & XENOPHONTOS, C. (eds) *Ophiolites. Oceanic Crustal Analogues*. Geological Survey Department, Nicosia, 149–163.

HÉBERT, R., SERRI, G. & HÉKINIAN, R. 1989. Mineral chemistry of ultramafic tectonites and ultramafic to gabbroic cumulates from the major oceanic basins and Northern Apennine ophiolites (Italy)—a comparison. *Chemical Geology*, **77**, 183–207.

HOECK, V. & KOLLER, F. 1999. The Albanian ophiolites and the Dinaride—Hellenide framework. EUG 10 Strasbourg. *Journal of Conference Abstracts*, **4**, 406.

HOECK, V., KOLLER, F., MEISEL, T., ONUZI, K. & KNERINGER, E. 2002. The Jurassic South Albanian ophiolites: MOR– vs. SSZ-type ophiolites. *Lithos*, **65**, 143–164.

INSERGUEIX-FILIPPI, D., DUPEYRAT, L., DIMO-LAHITTE, A., VERGÉLY, P. & BÉBIEN, J. 2000. Albanian ophiolites. II—Model of subduction zone infancy at a mid-ocean ridge. *Ofioliti*, **25**(1), 47–53.

ISPGJ–FGJM–IGJN 1983. *Harta gjeologjike e Shqiperise. Scale 1:200 000*. Tirana.

JONES, G., ROBERTSON, A. H. F. & CANN, J. R. 1991. Genesis and emplacement of the supra-subduction zone Pindos ophiolite, northwestern Greece. *In*: PETERS, T. NICOLAS, A. & COLEMAN, R.G. (eds) *Ophiolite Genesis and Evolution of the Oceanic Lithosphere*. Ministry of Petroleum and Minerals, Sultanate of Oman, 771–799.

KAMENETSKY, V. S., CRAWFORD, A. J., EGGINS, S. & MÜHE, R. 1997. Phenocryst and melt inclusion chemistry of near-axis seamounts, Valu Fa Ridge, Lau Basin: insight into mantle wedge melting and the addition of subduction components. *Earth and Planetary Science Letters*, **151**, 205–223.

KAMENETSKY, V. S., CRAWFORD, A. J. & MEFFRE, S. 2001. Factors controlling chemistry of magmatic spinel: an empirical study of associated olivine, Cr-spinel and melt inclusions from primitive rocks. *Journal of Petrology*, **42**(4), 655–671.

KLEIN, E. M. & KARSTEN, J. L. 1995. Ocean-ridge basalts with convergent-margin geochemical affinities from the Chile Ridge. *Nature*, **374**, 52–57.

KOMOR, S. C., ELTHON, D. & CASEY, J. F. 1985. Mineralogic variation in a layered ultramafic cumulate sequence at the North Arm Mountain Massif, Bay of Islands ophiolite, Newfoundland. *Journal of Geophysical Research*, **90**(B9), 7705–7736.

LETERRIER, J., MAURY, R. C., THONON, P., GIRARD, D. & MARCHAL, M. 1982. Clinopyroxene composition as a method of identification of the magmatic affinities of paleo-volcanic series. *Earth and Planetary Science Letters*, **59**, 139–154.

LOUCKS, R. R. 1990. Discrimination of ophiolitic from nonophiolitic ultramafic–mafic allochthons

in orogenic belts by the Al/Ti ratio in clinopyroxene. *Geology*, **18**, 346–349.

LUGOVI, B., ALTHERR, R., RACZEK, I., HOFMANN, A. W. & MAJER, V. 1991. Geochemistry of peridotites and mafic igneous rocks from the Central Dinaric Ophiolite Belt, Yugoslavia. *Contributions to Mineralogy and Petrology*, **106**, 201–216.

MECO, S. & ALIAJ, S. 2000. *Geology of Albania*. Beiträge zur regionalen Geologie der Erde, **28**. Borntraeger, Berlin.

MEISEL, T., SCHÖNER, N., PALIULIONYTE, V. & KAHR, E. 2002. Determination of rare earth elements (REE), Y, Th, Zr, Hf, Nb and Ta in geological reference materials G-2, G-3, SCo-1 and WGB-1 by sodium peroxide sintering and ICP-MS. *Geostandards Newsletter*, **26**(1), 53–61.

MÉTRICH, N. & RUTHERFORD, M. J. 1998. Low pressure crystallization paths of H_2O-saturated basaltic–hawaiitic melts from Mt. Etna: implications for open-system degassing of basaltic volcanoes. *Geochimica et Cosmochimica Acta*, **62**(7), 1195–1205.

MONZIER, M., DANYUSHEVSKY, L. V., CRAWFORD, A. J., BELLON, H. & COTTON, J. 1993. High-Mg andesites from the southern termination of the New Hebrides island arc (SW Pacific). *Journal of Volcanology and Geothermal Research*, **57**, 193–217.

MOORES, E. M., ROBINSON, P. T., MALPAS, J. & XENOPHONOTOS, C. 1984. Model for the origin of the Troodos massif, Cyprus, and other mideast ophiolites. *Geology*, **12**, 500–503.

MOORES, E. M., KELLOG, L. H. & DILEK, Y. 2000. Tethyan ophiolites, mantle convection, and tectonic 'historical contingency': a resolution of the 'ophiolite conundrum'. *In*: DILEK, Y., MOORES, E., ELTHON, D. & NICOLAS, A. (eds) *Ophiolites and Oceanic Crust: New Insights from Field Studies and the Ocean Drilling Program*. Geological Society of America, Special Papers, **349**, 3–12.

NICOLAS, A., BOUDIER, F. & MESHI, A. 1999. Slow spreading accretion and mantle denudation in the Mirdita ophiolite (Albania). *Journal of Geophysical Research*, **104**, 15155–15167.

NIMIS, P. 1995. A clinopyroxene geobarometer for basaltic systems based on crystal-structure modeling. *Contributions to Mineralogy and Petrology*, **121**, 115–125.

NIMIS, P. 1998. Clinopyroxene geobarometry of pyroxenitic xenoliths from Hyblean Plateau (SE Sicily, Italy). *European Journal of Mineralogy*, **10**(3), 521–533.

NIMIS, P. 1999. Clinopyroxene geobarometry of magmatic rocks. Part 2. Structural geobarometers for basic to acid, tholeiitic and mildly alkaline magmatic systems. *Contributions to Mineralogy and Petrology*, **135**, 62–74.

NIMIS, P. & ULMER, P. 1998. Clinopyroxene geobarometry of magmatic rocks. Part 1. An expanded structural geobarometer for anhydrous and hydrous, basic and ultrabasic systems. *Contributions to Mineralogy and Petrology*, **133**, 122–135.

NISBET, E. G. & PEARCE, J. A. 1977. Clinopyoroxene composition in mafic lavas from different tectonic settings. *Contributions to Mineralogy and Petrology*, **63**, 149–160.

PAMIĆ, J., TOMJLENOVIĆ, B. & BALEN, D. 2002. Geodynamic and petrogenetic evolution of Alpine ophiolites from central and NW Dinarides: an overview. *Lithos*, **65**, 113–142.

PARLAK, O., DELALOYE, M. & BİNGÖL, E. 1996. Mineral chemistry of ultramafic and mafic cumulates as an indicator of the arc-related origin of the Mersin ophiolite (southern Turkey). *Geologische Rundschau*, **85**, 647–661.

PARLAK, O., HÖCK, V. & DELALOYE, M. 2000. Suprasubduction zone origin of the Pozantı–Karsantı ophiolite (southern Turkey) deduced from the whole-rock and mineral chemistry of the gabbroic cumulates. *In*: BOZKURT, E., WINCHESTER, J. A. & PIPER, J. D. A. (eds) *Tectonics and Magmatism in Turkey and the Surrounding Area*. Geological Society, London, Special Publications, **173**, 219–234.

PARLAK, O., HÖCK, V. & DELALOYE, M. 2002. Suprasubduction zone Pozantı–Karsantı ophiolite, southern Turkey: evidence for high pressure crystal fractionation of ultramafic cumulates. *Lithos*, **65**, 205–224.

PARSON, L. M. & HAWKINS, J. W. 1994. Two-stage ridge propagation and the geological history of the Lau backarc basin. *In*: HAWKINS, J., PARSON, L., ALLAN, J. *et al.* (eds) *Proceedings of the Ocean Drilling Program, Scientific Results, 135*, Ocean Drilling Program, College Station, TX, 819–828.

PEARCE, J. A. 2003. Supra-subduction zone ophiolites: the search for modern analogues. *In*: DILEK, Y. & NEWCOMB, S. (eds) *Ophiolite Concept and the Evolution of Geological Thought*. Geological Society of America, Special Papers, **373**, 269–293.

PEARCE, J. A., LIPPARD, S. J. & ROBERTS, S. 1984. Characteristics and tectonic significance of suprasubduction zone ophiolites. *In*: KOKELAAR, B. P. & HOWELLS, M. F. (eds) *Marginal Basin Geology*. Geological Society, London, Special Publications, **16**, 77–94.

PUTIRKA, K. 1999. Clinopyroxene + liquid equilibria to 100 kbar and 240 kbar. *Contributions to Mineralogy and Petrology*, **135**, 151–163.

PUTIRKA, K., JOHNSON, M., KINZLER, R., LONGHI, J. & WALKER, D. 1996. Thermobarometry of mafic igneous rocks based on clinopyroxene–liquid equilibria, 0–30 kbar. *Contributions to Mineralogy and Petrology*, **123**, 92–108.

PUTIRKA, K. D., MIKHAELIAN, H., RYERSON, F. & SHAW, H. 2003. New clinopyroxene–liquid thermobarometers for mafic, evolved, and volatile-bearing lava compositions, with applications to lavas from Tibet and the Snake River Plain, Idaho. *American Mineralogist*, **88**, 1542–1554.

ROBERTSON, A. H. F. & SHALLO, M. 2000. Mesozoic–Tertiary tectonic evolution of Albania in its regional Eastern Mediterranean context. *Tectonophysics*, **316**, 197–254.

ROEDER, P. L. 1994. Chromite: from the fiery rain of chondrules to the Kilauea Iki lava lake. *Canadian Mineralogist*, **32**, 729–746.

ROSS, K. & ELTHON, D. 1993. Cumulates from strongly depleted mid-ocean-ridge basalt. *Nature*, **365**, 826–829.

SACCANI, E. & PHOTIADES, A. 2004. Mid-ocean ridge and supra-subduction affinities in the Pindos ophiolites (Greece): implications for magma genesis in a forearc setting. *Lithos*, **73**, 229–253.

SACCANI, E., BECCALUVA, L., COLTORTI, M. & SIENA, F. 2004. Petrogenesis and tectono-magmatic significance of the Albanide–Hellenide Subpelagonian ophiolites. *Ofioliti*, **29**(1), 75–93.

SCHMINCKE, H.-U., KLÜGEL, A., HANSTEEN, T. H., HOERNLE, K. & VAN DEN BOGAARD, P. 1998. Samples from the Jurassic ocean crust beneath Gran Canaria, La Palma and Lanzarote (Canary Islands). *Earth and Planetary Science Letters*, **163**, 343–360.

SERRI, G. 1981. The petrochemistry of ophiolite gabbroic complexes: a key for the classification of ophiolites into low-Ti and high-Ti types. *Earth and Planetary Science Letters*, **52**, 203–212.

SHALLO, M. 1992. Geological evolution of the Albanian ophiolites and their platform periphery. *Geologische Rundschau*, **81**, 681–694.

SHALLO, M. 1994. Outline of the Albanian ophiolites. *Ofioliti*, **19**(1), 57–75.

SHALLO, M. & DILEK, Y. 2003. Development of the ideas on the origin of Albanian ophiolites. *In*: DILEK, Y. & NEWCOMB, S. (eds) *Ophiolite Concept and the Evolution of Geological Thought*. Geological Society of America, Special Papers, **373**, 351–363.

SHALLO, M., KODRA, A. & GJATA, K. 1990. Geotectonics of the Albanian ophiolites. *In*: MALPAS, J. MOORES, E. M., PANAYIOTOU, A. & XENOPHONTOS, C. (eds) *Troodos 1987—Ophiolites, Oceanic Crustal Analogues*, 265–269.

SMITH, A. G. & RASSIOS, A. 2003. The evolution of ideas for the origin and emplacement of the western Hellenic ophiolites. *In*: DILEK, Y. & NEWCOMB, S. (eds) *Ophiolite Concept and the Evolution of Geological Thought*. Geological Society of America, Special Papers, **373**, 337–350.

STURM, M. E., KLEIN, E. M., KARSTEN, J. L. & KARSON, J, A. 2000. Evidence for subduction-related contamination of the mantle beneath the southern Chile Ridge: implication for ambiguous ophiolite compositions. *In*: DILEK, Y., MOORES, E. M., ELTHON, D. & NICOLAS, A. (eds) *Ophiolites and Oceanic Crust: New Insights from Field Studies and the Ocean Drilling Program*. Geological Society of America, Special Papers, **349**, 13–20.

TARTAROTTI, P., SUSINI, S., NIMIS, P. & OTTOLINI, L. 2002. Melt migration in the upper mantle along the Romanche Fracture Zone (Equatorial Atlantic). *Lithos*, **63**, 125–149.

TAYLOR, W. R. 1998. An experimental test of some geothermometer and geobarometer formulations for upper mantle peridotites with application to the thermobarometry of fertile lherzolites and garnet websterite. *Neues Jahrbuch für Mineralogie, Abhandlungen*, **172**, 381–408.

TUCHOLKE, B. E., LIN, J. & KLEINROCK, M. C. 1998. Megamullions and mullion structure defining oceanic metamorphic core complexes on the Mid-Atlantic Ridge. *Journal of Geophysical Research*, **103**, 9857–9866.

YANG, H.-J., KINZLER, R. & GROVE, T. L. 1996. Experiments and models of anhydrous, basaltic olivine–plagioclase–augite saturated melts from 0.001 to 10 kbar. *Contributions to Mineralogy and Petrology*, **124**, 1–18.